Gait Recognition using Time of Flight Sensor

Hazem Ali

2011/06/30

Abstract

Motion capture and analysis has an important role in many fields, therefore it has been for long time and still is an active research field. A large number of applications can benefit from motion capture and analysis, including athlete training, medical diagnostics, surveillance, and video retrieval. Conventional motion capture relies on attaching sensors or markers to the subject's body. While most recent motion capture approaches are markerless and try to extract biomechanical models and features, based on non-intrusive techniques such as video based approach. This project aims to develop a video analysis system for extracting gait features based on depth and intensity frames acquired by Time-of-Flight (ToF) camera . The main steps of the project are as follows: Segmentation to extract body silhouettes from frames using depth information provided by the 3D ToF camera which represents the distance from the object to the camera for every pixel in the intensity frames. After that we apply morphological filters to enhance the segmented object and eliminate the background noise. The enhanced silhouette is then divided into body segments based on human anatomical knowledge. Then we apply ellipse fitting techniques on the body segments to obtain a set of topological features of the silhouette. The resulting gait pattern representing the evolution of these topological parameters in time is called the gait pattern or signature and used to characterize the gait of a person. Once these signatures are obtained for every subject in the test group, we conduct several tests of robustness of their signatures for identification. The results obtained so far show very good recognition rates. This master thesis has resulted in one conference paper in BIOSIG 2011.

Preface

This thesis is dedicated to the memory of my father, who showed me the way and how to be strong against the tough conditions. It is also dedicated to my mother, sisters, brothers and lovely daughters for their support and encouragement along the way. The realization of this work was only possible due to the several people's collaboration, to which desire to express my gratefulness. First of all i would like to thank my supervisor Dr. Faouzi Alaya Cheikh for his endless support and useful instructions, advices, and interesting feedback. My thanks to Mohammed Derawy for his help during this thesis especially in the analysis part. I want to extend my gratitude to all my teachers in Gjøvik university college. I really appreciate the participation of the volunteers in the experiments, Without their help this work would never been done. My last but not least thanks goes to the municipality of gjøvik for allowing me to complete my two years study as part of introduksjonsprogram.

Hazem Ali, 2011/06/30

Contents

List of Figures

List of Tables

1 Introduction

This master degree project will develop a gait recognition system based on time of flight sensor. The system aims to provide a tool to recognize people by their gait. Gait is defined as "*The manner or style of walking, including rhythm, cadence, and speed.*" [1]. Most of human activities involve movements, which can be described in time and space. Video based biomechanical analysis of human motion typically rely on analysis of each from each frame of a video sequence in the spatial domain to extract the needed features and in time domain to determine the evolution of these features in the sequence of frames. The evolution of the extracted features in time characterizes the human gait movement.

1.1 Topics covered by the project

The main topics covered in the project are first, a review of biomechanical concepts and parameters which characterize the human gait. This is the background of human motion analysis in which the human body is modeled as rigid segments connected with joints. The second main issue covered in this project is image segmentation. The accurate segmentation of the subject in each frame of the sequence is followed by feature extraction process. Thresholding, which yields a binary image used for segmentation, thanks to the relative depth information obtained from the ToF camera. The resulting image is further processed using morphological operations such as dilation, erosion and connected component labeling to reduce noise and improve the quality of the segmented object. Ellipse fitting used to extract the segmented body parts comes and as the third issue. The next topic is the identification of gait features in the individual images to characterize the gait features evolution in time which represents the gait signature that can be used to recognize people.

1.2 Keywords

Video analysis, 3D, time-of-flight, authentication,recognition, identification, verification, biometrics, gait , biomechanics, joint angles, feature, signature, pattern, ellipse.

1.3 Problem description

Motion capture and analysis has an important role in many fields therefore it has been and is still an active research area. It has applications in analysis of human gait, athlete training, medical diagnostics,rehabilitation, surveillance, and video retrieval. Conventional motion capture approaches may be grouped in three groups: the first, to attach sensors to the joints of human body to record the position of each joint at every moment. The problem with such approach is that it is labor intensive, and requires professional users of the system as wrong placement of the sensors can lead to wrong data acquisition. Another drawback of such system is its intrusiveness and time consumption. To mount the sensors on the subject's body can take up to one hour. The second group of techniques uses floor sensors in which reaction forces are measured

[2, 3, 4]. While this technology has the advantage of being unintrusive, it has the drawback of the limited parameters that can be measured. The third group proposes to analyze a video [5, 6], which can be with or without markers. Marker-based systems require mounting markers on the subject's body landmarks such as joints, multiple cameras are used to calculate the relative marker location using triangulation [7] to build model of subject's body in 2D/3D. Active marker systems [8, 9, 10] use a number of light emitting diodes (LED), or passive markers retroreflective [11, 12]. The main advantage of marker based systems is its high accuracy, but it has drawbacks, such as, markers can be occluded or missed in the tracking process, attaching the markers is time consuming. Markers are obtrusive such that, it can limit the subject's movement. Due to the mentioned drawbacks marker based systems applications are limited to clinical and sports applications. Markerless systems are based on image processing techniques to find the required natural markers on the body and to track them. Markerless motion analysis can be model-based [13, 14, 15],or model-free [16, 17, 18, 19]. The main advantages of markerless based system is unobtrusiveness, simplicity and cost effective. On the other hand it is not as accurate as marker-based systems, and requires complicated feature extraction algorithms which increases the computational cost. In this project we propose a markerless approach to develop unintrusive system that requires no cooperation from the monitored people. The prototype system we propose includes the following modules: 1) video acquisition using ToF camera, 2) feature extraction from video frames, 3) correspondence between the features of every frame to construct feature vectors, 4)Similarity measurement between these feature vectors.

1.4 Justification, motivation and benefits

The gait is characterized by kinematics [20]. Static and dynamic features such as speed, stride length, cadence rate, and angular and linear displacements of body segments can be extracted by biomechanical analysis of walking human body. Psychophysical studies [21, 22, 23] showed that people can recognize/identify friends, and gender from the way they walk. Gait as a biometric feature has gained increasing attention, as it can be collected from a distance using a video camera. In controlled environments like work places, banks and airports it is preferred to use non-intrusive authentication methods. After obtaining gait features using ToF camera, classification techniques can be applied on the feature vectors to compare the different subjects' gait patterns. This project aims to develop biomechanical analysis system to extract gait patterns from walking subject's videos acquired by ToF camera. In this project our experiments will focus on walking subjects in controlled environment, to capture their movements in a constrained distance from the camera. One camera is placed on the side of the track to record the subjects walking. The prototype systems we propose can extract the required gait features automatically from the video sequences acquired by the ToF camera. We propose to develop an integrated gait analysis and recognition system, which requires no cooperation from the subjects and no human intervention can be part of identity verification or security system.

1.5 Research questions

The research work in this project tries to answer the following questions:

1. To what extent the time-of- flight camera provides a good segmentation tool ?

2. How to extract accurate biomechanical parameters from ToF video sequence?
3. What are the main biomechanical parameters that can be used for gait based identification?
4. How to characterize a gait pattern form a ToF camera by a signature and how to compare them?
5. Are recognition rates consistent over time?

1.6 Planned contribution

The planned contribution of this master project is to develop an automatic system for video-based gait analysis, and use it to recognize people. The main goal is to extract useful biomechanical information from the video sequences of a walking subject. For an input video captured by a ToF camera, depth information is used to segment subject's body from the video sequence. The segmented body silhouettes are fed to the feature extraction step, some critical kinematic parameters of action are automatically obtained through this component of the system, and finally pattern recognition step. In which different gait signatures are compared to identify subjects. Therefore, the steps can be summarized as follows:

1. Body segmentation from the video.
2. Biomechanical features extraction and the representation of their evolution in time.
3. Detection of specific patterns in these representations (characteristic patterns of gait).
4. Comparison of these patterns to recognize people by gait.

1.7 Choice of methods

The project has been divided into four phases. We used both literature and experimental methods to complete the project. In the first phase we will review the literature to identify the previous research activities related to the project. This phase is essential to provide us with comprehensive information to define what and how gait features can be extracted. In the second phase a prototype system is implemented to capture intensity and depth data from MESA's [24] SR4000 TOF sensor and analyze video to extract the gait features. Using depth images the subject is extracted from the background, feature extraction algorithm is applied to extract the lower limbs inclination angles. The adopted methodology for the third phase is carrying out experiment. The goal of the experiment is to verify the validity and robustness of the proposed system. This is best done in a lab environment where one has more control over the environment. The experiment is done in the lab and about 30 people participate in the experiment for two sessions to validate the robustness of the extracted features over time. The fourth phase is the statistical analysis of the experiment data, in which the data of each session is used separately to identify the subjects, in a second phase the data of the two sessions is used to carry out over-time recognition test to check the robustness of the proposed recognition approach over time.

2 Introduction to biometric authentication and gait

2.1 Biometric Authentication

Authentication is the process of determining that a person are whom he/she claimed to be. In the context of information security this can be done through authentication factor. This factor can be a password or PIN (something the user knows), or the possession of physical object like a smart card and one time password (OTP) tokens, in the recent years a third category was added to the first two called biometric authentication. Biometrics are physiological like finger print, retina and iris or behavioral like gait and voice. As the number of applications we are using increases, the number of password we need memorize increases, which is a hard task to handle, additionally smart cards and tokens are susceptible to loss or theft. For this reasons biometrics gained a lot of attention, as it can not be stolen or forgotten.

2.1.1 Authentication system structure

A authentication system is built of four units:

1. User Interface, which can be a sensor, key board or smart card reader to submit the authentication factor.
2. Feature extraction module, in which the recognition features are extracted from the input data like fingerprint, iris scan etc.
3. Quality checker, this modules controls the quality of the acquired data.
4. Matching unit, in which the extracted features are compared to the stored templates.
5. System database, used to store all the enrolled users' templates.

The authentication process is composed of two main actions, as illustrated in figure 1. First, enrollment mode in which the user becomes known to the system by acquiring the authentication factor for the enrolled person. Secondly, the identification / verification action. In identification mode, the user is identified from the enrolled population using the authentication factor submitted by the user by searching the templates already stored in the system's database (one-to-many). In verification mode a user is compared with his own previously enrolled template. The comparison between two templates results a similarity measure called matching score of the compared templates. According to a preset threshold value, the system determines the tolerance to classify a user as genuine or impostor. The system's accuracy is sensitive to the threshold value. A small threshold value will result in high false matching rates, and high threshold might result in false non-matching (high rejection rate).

2.1.2 Errors and their measurement

Authentication system performance is evaluated according to its recognition speed and accuracy. Biometric systems are never perfect, and error prone. These errors can occur in any stage of the

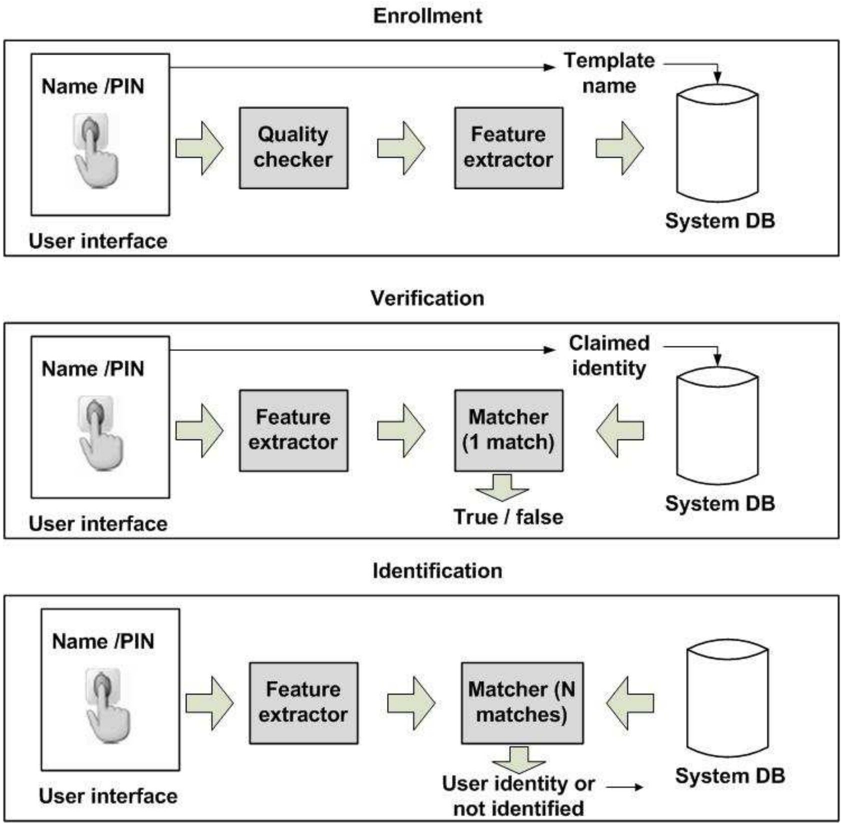

Figure 1: Block diagram of a typical authentication process [25].

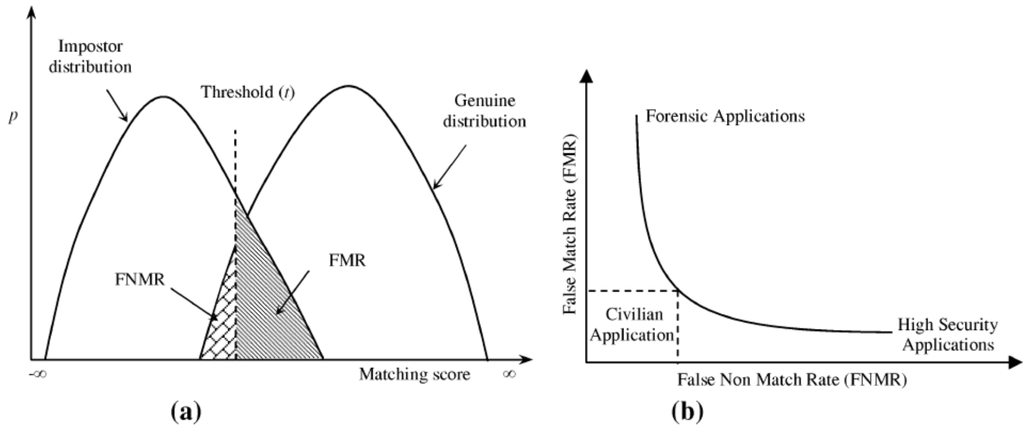

Figure 2: Biometric system errors [25].

authentication process. The error rates are in any authentication system are estimated statistically, as their is no theoretical computation foundation to calculate it [26]. The different errors in the authentication systems are :

Fail to enroll rate (FTE)

The interaction with a biometric system starts with enrollment of the users. FTE measures the probability that a user is unable to enroll to the system.

Fail to acquire rate (FTA)

In identification/ verification if the acquired data does not meet the quality requirement of the system, as a result the collected sample is not usable for matching and the user can't be identified. FTA is the probability that the collected sample does not march quality criteria of the system.

Matcher errors

Matching process is error prone due to many reasons including sensors' accuracy variabilities and users' way of presenting the biometrics. For a pair of samples, the probability of match is called genuine distribution and the probability of non-match is called impostor distribution, see figure (2-a). The matching process is influenced by the threshold value of the matching score, the threshold value can yield two types of errors: false match rate (FMR) in which two samples from two different users are mistakenly counted as a match, and false non-match rate (FNMR), in which sample pair of a user are mistakenly counted as non-match. The system's performance is function of FMR and FNMR , according to the application of the system a threshold trade-off is made. The proper threshold is found using receiver operating characteristic curve (ROC)[27]. ROC is a plot of FMR versus FNMR for various threshold values, see figure (2-b).

False acceptance rate (FAR) is the probability that an intruder is identified by the matcher as legitimate user and it is caused by a false match, False rejection rate (FAR) is the probability that an genuine user is rejected by the matcher genuine user and it is caused by a false non match, FAR and FRR are controlled by changes in the threshold value. The point where FAR and FRR are equal is called Equal Error Rate(EER), and is used as system's performance measure.

2.1.3 Biometric Systems

Biometrics are defined as measurements of biological phenomena or physical characteristic. Any human physiological or behavioral characteristic is counted as a biometrics if it meets the following criteria:

- Universality: Each individual should have the characteristic.
- Uniqueness: No pair should have the same characteristic.
- Permanence: Consistency of a biometric over a certain period of time.
- Collectability: ease of acquisition for measurement.

Biometric system uses pattern recognition technologies to identify individuals based biometrics. Biometric identifiers are most commonly used as part of a multi-factor authentication system, combined with a password (something a person knows) or a token (something a person has). Various biometric techniques and identifiers are being developed and tested, the quality of biometric systems depends on:

- Performance: accuracy, speed, and robustness of technology used.
- Acceptability : The extent to which people accept to provide such a characteristic for identification.
- Circumvention : ease of fooling the system.

2.1.4 Overview of commonly used biometrics

The biometric authentication is based on a number of human behavioral and physiological characteristic listed below:

Fingerprint

Fingerprint-based identification has been successfully used since the nineteenth century [28]. Everyone is known to have unique, unchangeable fingerprints. A fingerprint is made of a series of unique ridges and furrows on the surface of the finger. These features are consistent over time except in case of injury and manual workers. Finger print scanners are cheap and widely used in many applications for identification and verification.

Infrared thermogram (facial, hand, and hand vein)

Infrared thermogram uses infrared camera to captures the human's body radiation pattern created by the branching of blood vessels and emitted from the skin. These patterns, called thermograms, are highly distinctive.It's advantages as biometric technology are that it is not intrusive and no physical contact is required. The draw back of this technology is that it is highly sensitive to surround temperature, acquiring such image in uncontrolled environment is highly challenging.

Face

One of the most used biometrics for person recognition. Face features are extracted from images (static and dynamic), these features can be the shape or location of some local facial attributes like eyes, eyebrows, nose. Face recognition is very sensitive to lighting conditions, hair shape, or

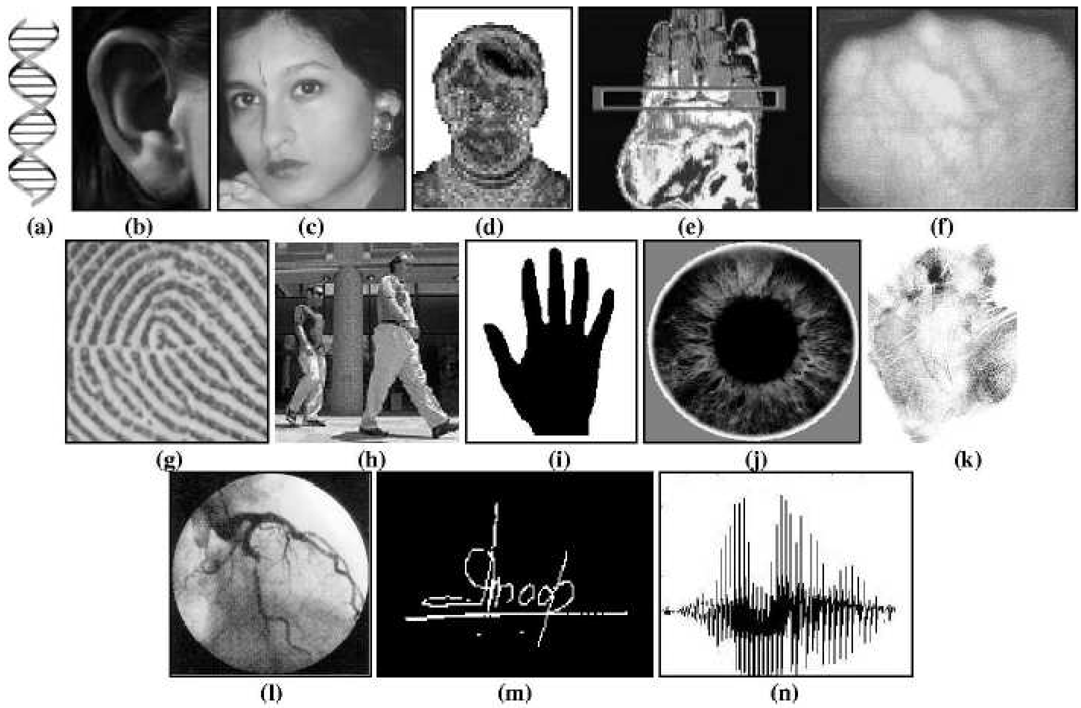

Figure 3: Example biometrics, (a) DNA, (b) ear, (c) face, (d) facial thermogram, (e) hand thermogram, (f) hand vein, (g) fingerprint, (h) gait, (i) hand geometry, (j) iris, (k) palmprint, (l) retina, (m) signature, and (n) voice [25].

other objects partially covering the subject's face like sunglasses.

Voice

The voice is created by invariant physical features such as vocal tracts, mouth, nasal cavities and lips, but it also has a behavioral aspect. The behavioral part of the voice is not consistent over long period of time and it can be changed due to aging, medical conditions and emotional state.

Keystroke

Keystroke dynamics is a behavioral biometric, the hypothesis behind this biometric is that each person types on a keyboard in a unique characteristic way.

Signature

Signature is a behavioral characteristic of individuals which can vary over time and also influenced by the person's physical and emotional conditions. The signature reflects the uniqueness of signatories hand geometry. Signatures are accepted by governments and banks as a biometric although it can be forged sometimes.

Hand geometry

Hand geometry is a simple biometric which employs the geometric feature of the hand and fingers like the location of joints, shape and size of palm. It is not very distinctive for large population, therefore it is used in verification rather than identification.

Retinal scan

The retina has a complex vascular structure which is supposed to be unique and time invariant for healthy people. the retinal scan is acquired using near infrared scanner which requires full cooperation from the subject, that's why it is not widely accepted by the public.

Iris scan

The iris scan is image acquisition of the colored area around eyes pupil which can be acquired without subject cooperation even if the subject wears contact lenses or glasses. The iris contains a complex texture patten which is thought to be unique even for twins.

Odor

Each subject exudes an distinctive chemical composition (odor), this biometric system based on chemical sensors, each of them is sensitive to a group of compounds in order to recognize people. Deodorants and perfumes can reduce the performance of such systems.

Ear

The human ear is a new feature in biometrics. The ear has relatively stable structure over time which is suggested to be distinctive, it can be easily captured from a distance without subject's cooperation, but it can be hidden with hair, scarf and jewelery. Ear based recognition matches the distances of salient points on the pina from a landmark location of the ear.

DNA

Deoxyribonucleic acid (DNA) is ultimately unique code for each person, except for identical twins. DNA as biometric has some limitation for authentication: 1) contamination and sensitivity: it is easy to steal and use for ulterior purpose; 2) present technology for DNA matching requires complicated chemical methods which requires skilled experts, therefore it is not suitable for online applications 3) taken DNA samples may reveal information about the susceptibility to certain diseases and misuse of this information leads to privacy breach. Therefore the usage of DNA is limited to forensic applications. Each of the above mentioned biometrics has its pros and cons, which limits it to a certain set of applications, table 1 summarizes the properties of each of these biometrics as high, medium and low.

Biometric characteristic	Universality	Distinctiveness	Permanence	Collectability	Performance	Acceptability	Circumvention
Facial thermogram	H	H	L	H	M	H	L
Hand Vein	M	M	M	M	M	M	L
Gait	M	L	L	H	L	H	M
Keystroke	L	L	L	M	L	M	M
Odor	H	H	H	L	L	M	L
Ear	M	M	H	M	M	H	M
Hand Geometry	M	M	M	H	M	M	M
Fingerprint	M	H	H	M	H	M	M
Face	H	L	M	H	L	H	H
Retina	H	H	M	L	H	L	L
Iris	H	H	H	M	H	L	L
Palmprint	M	H	H	M	H	M	M
Voice	M	L	L	M	L	H	H
Signature	L	L	L	H	L	H	H
DNA	H	H	H	L	H	L	L

Table 1: Comparison of various biometric technologies [25].

2.2 Gait

The study of human gait as a biometric started more than fifteen years ago [29]. The gait is considered to be as a total walking cycle, "*for normal gait, the duration of successive temporal components and the length of successive steps are rhythmic*" [20]. It is also described by*[30]*, as a discriminatory set of features includes individual’s weight, limb length, footwear, and posture combined with characteristics of motion. Therefore, gait has the basic characteristics needed in a biometric , to identify or verify people. The gait is sensitive to many covariant conditions which can affect the gait characteristic during walk, in terms of walking speed, step and stride length, and cadence rate. Type of footwear, clothing walking carrying-condition have strong influence on gait pattern [31, 32, 33]. Gait analysis depends on extracting the related kinematic features using, machine vision (MV) which employs image processing techniques, wearable sensors (WS) with acceleration variation during gait as a discriminatory feature, and floor based sensors (FS) where reaction forces applied on the foot are measured. The most widely used technique is based on MV, but this method is sensitive to filming view angle and subject's clothing. Gait based human recognition relies on measuring the similarity of the extracted features from different subjects, therefore, the gait analysis system should take into account the different covariant conditions such as, shoes, view angle, and clothing.

2.2.1 Gait cycle

The gait cycle is composed of main phases, stance and swing [34]. The stance phase is the period where the foot is in contact with the ground and equates to 60% of the cycle when walking, see figure 4.

Stance

- Heel strike - The point when the heel hits the floor
- Foot flat - The point where the whole of the foot comes into contact with the floor
- Mid stance - Where we are transferring weight from the back, to the front of our feet
- Toe off - Pushing off with the toes to propel us forwards

Swing

- Acceleration - The period from toe off to maximum knee flexion in order for the foot to clear the ground
- Mid-swing - The period between maximum knee flexion and the forward movement of the tibia (shin bone) to a vertical position
- Deceleration - The end of the swing phase before heel strike.

When running, a higher proportion of the cycle is swing phase as the foot is in contact with the ground for a shorter period. Because of this there is now no double stance phase, and instead there is a point where neither feet are in contact with the ground, this is called the flight phase. As running speed increases, stance phase becomes shorter and shorter.

2.2.2 Gait features

The extensive research activity on gait analysis for recognition and clinical purposes resulted in a large set of features to characterize the human gait signature. Extraction of kinematic that describe body movements during gait, relies on: dynamic features locating the coordinates of points such as hip joint, knee, and foot and tracking them in each frame [15, 36, 37]. The data is modeled according to biomechanical structure of the human body in order to analyze it and form the gait signature. Static features related to body geometry such as height and length and width of different body segments [38]. combination of static and dynamic gait features is used to achieve better recognition rate [14, 39, 40, 41]. Dynamic features based experiments achieved higher recognition rates [42, 20]. Human gait can be characterized by large number of

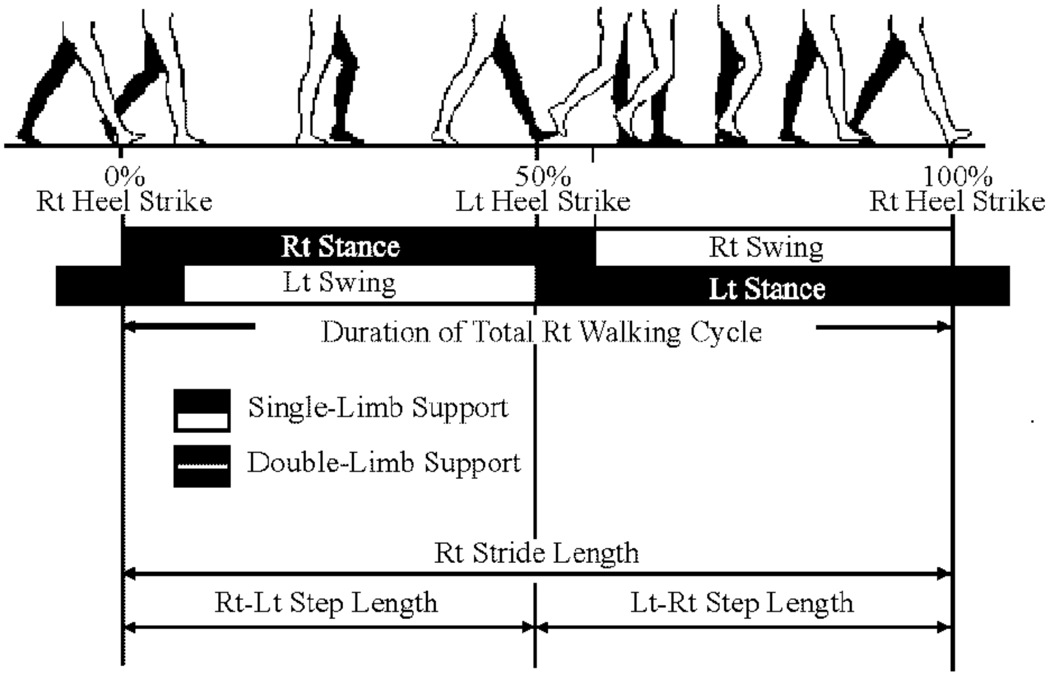

Figure 4: Gait cycle [35].

parameters table 2 summarizes the most used ones.

Parameter	Definition
Stride length	The distance between ground contact of one foot and the subsequent ground contact of the same foot
Step length	The distance between ground contact of one foot and the subsequent ground contact of the opposite foot
Step width	The perpendicular distance between similar points on both feet measured during two consecutive steps
Absolute angles	The orientation of a body segment in space (Trunk, thigh, shin and foot), the angle of inclination of a body segment measured from the right horizontal placed at the distal end of the segment.
Relative angle	The joint angle; the included angle between the longitudinal axes of two adjacent segments such as hip, knee and ankle
Stride time	Time in seconds from ground contact of one foot to ground contact of the same foot
Speed	Distance/time, usually reported in m/sec
Cadence	Steps per minute

Table 2: Gait parameters.

3 Related work

3.1 Introduction to motion analysis systems

Biomechanics is the area of science where the laws, principles and methods of mechanics are applied to the structure and function of the human body. Mechanics can be divided into two categories: statics, which is the study of stationary objects, and dynamics, which is the study of moving objects. Most activities in sport involve movement and therefore require the application of dynamics to understand that movement. Dynamics which is often used to describe different levels of biomechanical analysis, has two subdivisions: Kinematics, which is a description of the movement in terms of time and space, and kinetics, which is concerned with an explanation of the underlying mechanics of the movement and typically involves an assessment of forces. Biomechanical analysis of motion typically rely on two sources. Images; which can be analyzed using image processing techniques to extract biomechanical parameters to describe certain human activity. The other source is the data acquired from different sensors which can be attached to subject's body, or like force plates that allow the measurements of the exerted forces against the ground during different activities.

3.1.1 Mechanical

The mechanical goniometers have been used in biomechanical applications. Micera et al [43] introduced a wearable mechatronic system, the prototype was composed of a two degree of freedom (DoF) exoskeletal structure connected to three independent elastic cloth parts and wireless magnetic sensors, to measure kinematic of the knee.The results obtained by the systems showed high correlation to the results obtained by passive marker optical system. It was evident that the system like electrogoniometer and similar exoskeletal devices were only capable of measuring angles in selected joints, and not in supplying complete kinematic information of motion. Also, the system showed the same disadvantage like goniometers, the alignment with body joints is a difficult task, especially when measuring multiple DoFs joints, like shoulder. Electrogoniometer were used in the work of Lindinger et al. [44] to study control of speed in double poling to measure elbow, hip, and knee angles during the different phases of the skier's activity.

3.1.2 Magnetic

Magnetic motion capture systems utilize small sensors placed on the body to measure the magnetic fields generated by a transmitter source in real time. The 3D sensors measure the strength of those fields and calculate position and orientation of each sensor based on its nine measured field values. Magnetic sensors can be aligned to the body accurately for full body capture, the main limitations of the magnetic sensors that its wired and sensitivity to ferrite materials in the surrounding. Kobashi et al. [45] used inertial and magnetic wearable sensors, the joint movement was measured using two of these sensors one for each of the body segments composing the joints. The proposed system was applied to evaluation of knee kinematics, and the evaluation experiments validated that the proposed system obtained flexion/extension angle with a mean error of -1.61 ± 3.09 deg; internal/external rotation angle of 0.93 ± 1.75 deg; and varus/valgus angle of 1.83 ± 1.79 deg. Ascension Technology Corporation in the United States [46] developed a magnetic sensing system with good performance with translation range: 3:05 m; angular range: all attitude 1808 for azimuth and roll, 908 for Elevation; static resolution (position): 0.08 cm at 1.52 m range; and static resolution (orientation): 0.1 RMS at 1.52 m range.

3.1.3 Inertial

Inertial sensors provide special acceleration of a rigid body, while full information of segment's kinematic is obtained using a triaxial accelerometer. Practical inertial tracking of a rigid body is made possible by advances in miniaturized and micro-machined sensor technologies, particularly in silicon accelerometers and rate sensors. Sensors are placed on each body segments to be tracked. OHGI [47] proposed a system to measure human or equipment movement in sports activities. The system was used to measure the swimmer's stroke kinematics using their wrist acceleration and the angular velocity. The swimmer's triaxial wrist acceleration, the angular velocity and the stroke path in the crawl stroke obtained, the data was used to compare the performance of different athletes using dynamic time wrapping technique since the acquired data length can vary for different athletes.The system was also tested on golf swing .

3.1.4 Marker based

Optical systems use optoelectronic devices to track movements of a body by tracking markers aligned to a specific points on the subject's body segments. Stereo metric techniques correlate with common tracking points on the tracked objects (markers) in multiple images, and along with knowledge of camera setup, calculates position of a marker in fixed coordinate system. Optical systems offer comprehensive solution since they enable simple reconstruction in three spatial dimensions of a global coordinate system. There are some evident drawbacks of marker based methods that it constrains the body motion by the presence of skin markers and relative movement between the skin, where the markers are placed, and the underlying bone. Fuller et al. [48] examined the validity of using skin mounted markers to measure the three-dimensional kinematics of the underlying bone. Kinematic data obtained from marker arrays mounted on skeletal pins that were screwed directly into the bone were compared with data from markers and markers' arrays, mounted on the skin. They found that skin mounted markers inappropriate for representing the motion of the underlying bones, and further processing of the data is needed.

Active markers

Commercial optical active markers systems such as Optotrak are often considered as a "golden standard" in human motion analysis. Authors of [49] evaluated the accuracy of motion between two rotation boards using an Optotrak optical motion capture system. Tests of this commercial system showed good results; angular accuracy of 0.04° and linear accuracy of 0.03 mm. Another good example of commercial systems BTS SMART-Performance from BTS engineering [50], Qualisys [51] , and Coda [52], those systems are widely used in sports and medical motion analysis applications. research and development of active markers based techniques going on, Stancic et. al. [10] proposed a system based on set of 10 LEDs and a single high speed camera, the system was tested in controlled environment to analyze gait cycle. The system setup was complex, required wiring of the markers and precise calibration of the camera. In [9] a system for capturing motion data using active markers was proposed , the system constructs skeleton of the human body based on the marker locations without prior knowledge about the person's pose.

Passive markers

Optical tracking method based on use reflective marker (passive marker) attached to the participant. Cameras pick up the reflections from the markers. These systems automatically capture marker position. and most systems present 3D position-time data of markers in real time or near real time. The main limitation of passive markers are illumination sensitivity and time consuming deployment. Passive markers are also widely used in commercial motion tracking analysis systems ,motion analysis from [53], and Qualisys [51] are among the widely used systems in sports and biomedical analysis applications.

3.1.5 Markerless

Systems without markers provide lower accuracy, but benefits in simplicity of measurement, no need to bother the subject by attaching markers or wearable sensors , analysis can be carried out in 3D or 2D. Li et al. [54] developed a method for tracking without markers referring to athletes in diving action. The athlete motion was analyzed throughout the diving action, different joint angles and the diver's water entry angle were measured, which demonstrates a visual motion estimation technique that is able to recover articulated human body configurations in video sequences. The proposed system automatically segments the video sequence to extract the athlete action, segments the image to fit the athlete body to 2D model and finally extracts biometric information. Goffredo et al.[55] introduced new approach using Gauss-Laguerre transform domain for human movement analysis, the system was examined on sit-to-stand task, model of the human body composed of four body segments has been applied. The first segment includes trunk and upper limbs, the second represents the thighs, the third is the shanks, and the fourth corresponds to the feet. Each segment is modeled as a rigid nonextensible segment and is linked with the next through an ideal joint. In order to appropriately match the human body model, four natural markers are selected on shoulder, hip, knee, and ankle joint positions in the first frame of each video, single camera was used to capture the subject in the experiment. The system achieved good results compared to marker based system. Aravind Sundaresan and Rama Chellappa[56] used 8-16 camera multi cue system using iterated extended Kalman filter algorithm to estimate human pose. Zhu et al. [57] proposed a model based system for pose estimation using depth image captured by time of flight camera [58], the system based on extraction of multiple features of anatomical landmarks. Rosenhahn et al. [59] exploited motion constrain in their modeling of athletes interacting with sport equipment to estimate their poses, they used four cameras to simulate the athletes in 3D.

3.2 Gait analysis systems

The ability to use gait for people recognition and identification been known for a long time. The earliest research started by the sixties of the twentieth century, where studies from medicine [60] and psychology [23] proved that human gait has discriminative patterns from which individuals can be identified. It is however just in the last decade that gait as a biometric feature has been introduced, and from a technical point of view the gait recognition can be categorized in three different classes. Machine Vision (MV) which uses video from one or more cameras, to capture gait data and video/image processing to extract features. This method is often used in surveillance and forensics. Floor Sensors (FS) that use sensors installed in the floor are able to measure gait features such as ground reaction forces and heel-to-toe ratio when a person walks on them. This method is usually used in identification. Finally we have Wearable Sensors (WS) where the gait data is collected using body-worn sensors and this method is normally used to authenticate a person.

3.2.1 Floor sensors

The majority of (FS) were mainly designed for tracking purposes, however,gait recognition using these sensor showed good recognition rates. The magic carpet [61] is a 16 x 32 grid of piezoelectric wires, running across the carpet at a roughly 4” inter-wire pitch, is used to sense foot pressure and position. The LiteFoot [62] is another system developed in parallel with the magic carpet. It is a 1.76 meter square and 10 centimeters high floor element, filled with a matrix of 1,936 optical proximity sensors. It detects the feet location the total impact force of the feet on the floor. The floor has an embedded micro-controller that scans all sensors at 100Hz. The Z-tile system [63] has a modular design with a spatial resolution is 40 millimeters. Each Z-tile has an upper and lower circuit board. The upper has 20 prexels (an array of pressure-sensitive elements), individually covered by plubber (carbon particles with sizes between 300 and 600 microns), while the inside of a tile houses micro-controllers and connections. Each Z-tile has four connection points along its perimeter see figure 5 where data and electrical power can be transferred.

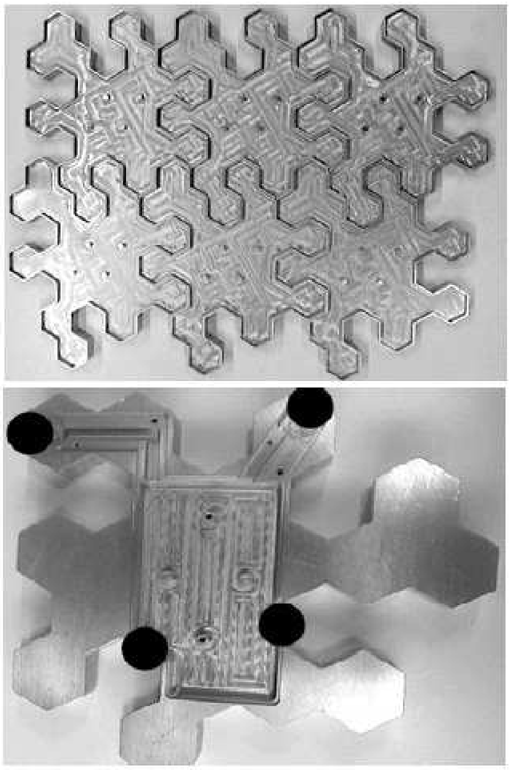

Figure 5: Z-tile [63].

Middleton et. al. [64] designed a system for gait recognition see figure 6, the system composed of 4 isolated sensor grids and 2 layers to enhance the spatial resolution of the system. For system evaluation they run an experiment with 15 subjects walking over the mat without shoes to alleviate the effect of the shoes on the experiment. They measured the stride length, stride cadence, and heel-to-toe ratio as gait features, they achieved 60% recognition rate using the heel-to-toe ratio, and 80% overall recognition rate. Smart floor system was introduced by Orr et. al. [65], it measures the ground reaction forces (GRF) of the subjects' feet as they step over the the measuring tile, the group have chosen 10 foot-step profile features as shown in figure 7. They used the nearest-neighbor search to match test data set with training set for 15 subjects participated in the experiment and achieved correct identification rate of 93%. The latest work was done by Qian et. al. [4] based on their previous work [66] were they used floor pressure sensing to identify people, in the fist experiment the subject were asked to work in straight line at normal speed to collect 1D pressure profile and 2D position trajectories of the centers of pressure (COP) of the subjects feet. 3D COP trajectories with stride length and cadence are used as feature set, Fisher linear discriminant is used as the classifier. They obtained average recognition rate of 94% and false alarm rate of 3% using pair-wise foot-step data from 10 subjects. for the later work the subjects were asked to walk freely by mean of speed and style over the sensing platform and they achieved an average recognition rate of92.3% and false alarm rate of 6.79%

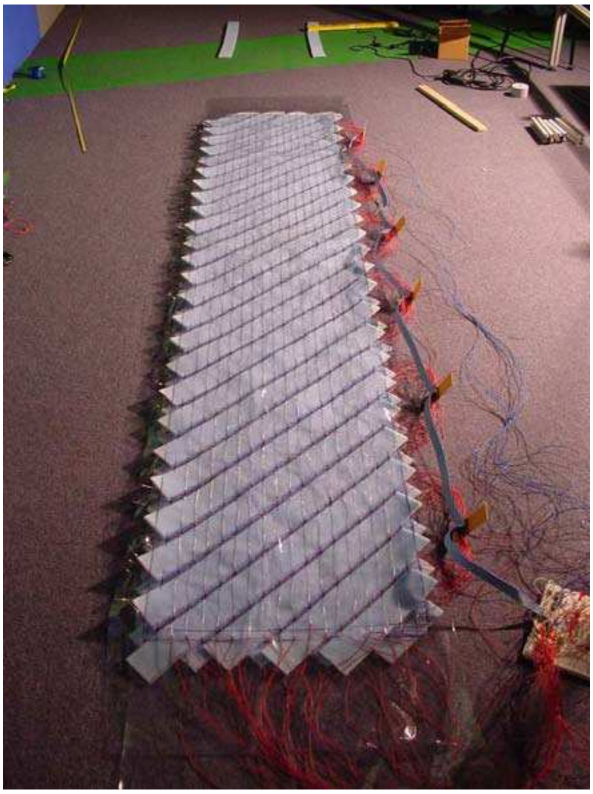

Figure 6: Sensor Mat[64].

using the best performing feature set.

3.2.2 Wearable sensors

In the last decades the warble sensor (WS) technologies have gained a lot of research interest, motivated by the evolution of the sensing technologies and the introduction of the new generation of personal digital assistants (PDA) and smart phones. The applications of WS are versatile and include clinical monitoring of individuals, and rehabilitation [67], motion analysis, athlete training, as well as security and authentication. WS can be a single accelerometer or accelerometers together with gyroscope to acquire biomechanical data, and can be worn in different places of the body such as ankle, hip, waist [68]etc. The acquired data are then used for classification of activities according to the application it is used for. Many of PDA's and smart phones have built in accelerometer which can be used to acquire acceleration data, the accelerometer was mainly attached to these devices to detect the orientation of the device and present the data accordingly. The availability of these accelerometers attracted many researchers to employ them in securing the devices like the different biometrics including voice, and finger prints which are already commercially in use. Ailisti et. al. [68] they were the first to use portable technologies for acquiring gait data using portable accelerometer worn on the subjects waist (from behind), see figure 8. They collected 3D acceleration data using laptop carried by the user, where x, y and

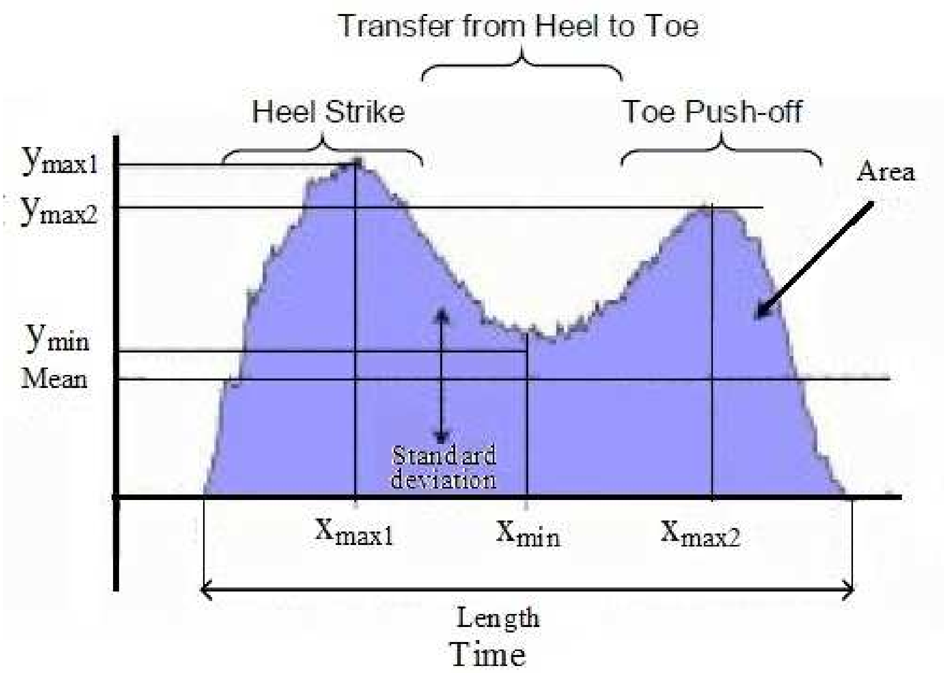

Figure 7: Footstep profile features[65].

z axes pointed forward, left and up respectively but in the analysis they used the x and z signals only, because the y acceleration data were not significant. The system was experimented by a set of 36 subjects for two sessions five days apart, by walking 20 meters. Using the correlation method to compare the gait templates. The results were as follows: the lowest total error rate (TER) is 12%, when false acceptance ratio (FAR) is 6.4% and false rejection rate (FRR) is 5.4%. The EER is 6.4%.

9.

Gafurov et.al. [69, 71, 70] carried out studies on WS's by acquiring 3D acceleration data from subjects, with sensors attached to hip and ankles of the subjects see figure 9. In [70] they attached the sensor to the subject's right leg to collect the acceleration data from 21 participants walking in normal speed for 70 meters. The collected data was separated into two sets one as enrollment sample and the other used for verification, they used two methods to compare the enrollment and verification data cycle length and histogram similarity and obtained EER of 9% and 5% respectively. In a study of robustness of gait based authentication [69] the acceleration signals was acquired from a sensor attached to the subject's hip, 22 volunteered in the experiment where 6 gait samples were collected for each subject. In the second session the subject's were paired and the partners in each pair were asked to imitate the others walking style. The imitated sample were compared with the targeted subjects only, the experiment EER was 16%. Rong et. al. [72] attached the sensor to the waist for 20 subjects who participated in the experiment and they used time and frequency domain analysis. They used cycle matching technique for recognition

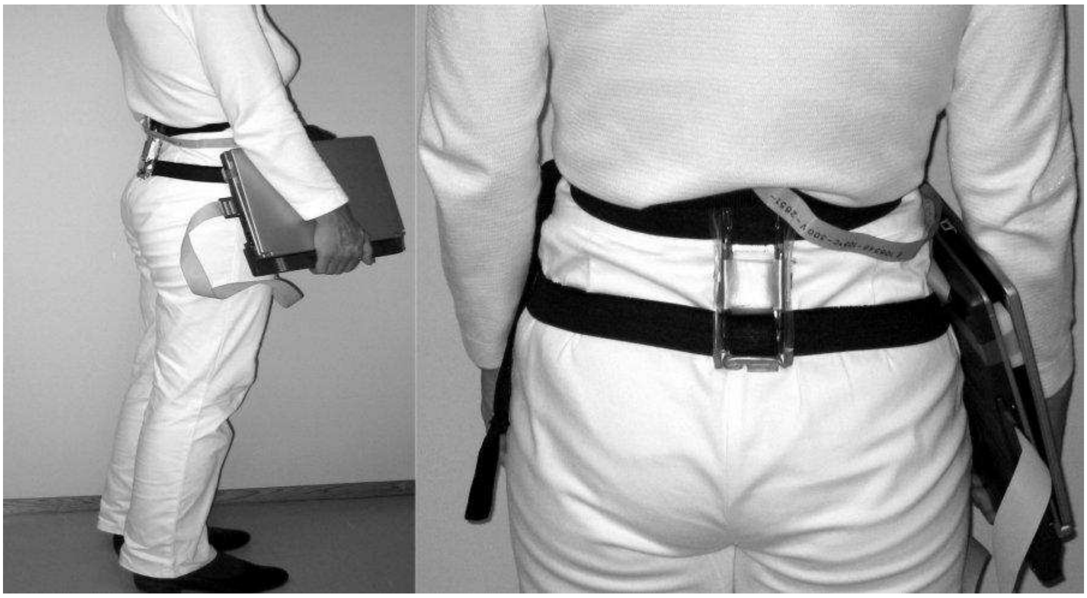

Figure 8: The experimental system for gait acceleration data collection [68].

(a) (b)

Figure 9: Attachment of the sensors (a) ankle (b)hip [69, 70].

Figure 10: Mobile phone attachment to subject's hip to measure acceleration in 3D [73].

employing dynamic time warping (DTW) to overcome the different cycle lengths of the collected data, and achieved EER of 5.6% for time domain and 21.1% for frequency domain. Using mobile phones' built-in accelerometers was studied in [73, 74, 75], The mobile phone was attached to the hip of the subject in the three works see figure 10. Using support vector machine (SVM) Sparger et.al. [75] achieved 92.9% recognition accuracy for data acquired at. Derawi et. al. [73] obtained EER of 20.1% using DTW, Nickel et. al. [74]results were better using 7-state hidden markov model (HMM) . The EER was approximately 10%.

3.2.3 Machine vision

Machine vision (MV) is the mostly used gait recognition technique, as it allows the collection of gait features from a distance. MV-based gait recognition is mainly used in surveillance and forensics applications [76, 77, 78]. In MV image processing techniques are used to extract static like stride length which are determined by body geometry [38], and dynamic features from body silhouettes. The MV-based gait analysis techniques can be classified as model-based [14, 15] and model free [16, 17, 18, 19]. The main advantage of model based approaches is the direct extraction of gait signatures from model parameters, but it is computationally expensive. Model free techniques characterize the body motion independently from the body structure. The MV gait analysis can also be categorized according to the technology, as marker-based and markerless. In marker based system specific points in the subject's body are labeled by markers by tracking these points in the video sequence the body motion can be tracked and analyzed [21, 37, 79]. The MV-based gait recognition provides wide range of gait features and many works utilized different

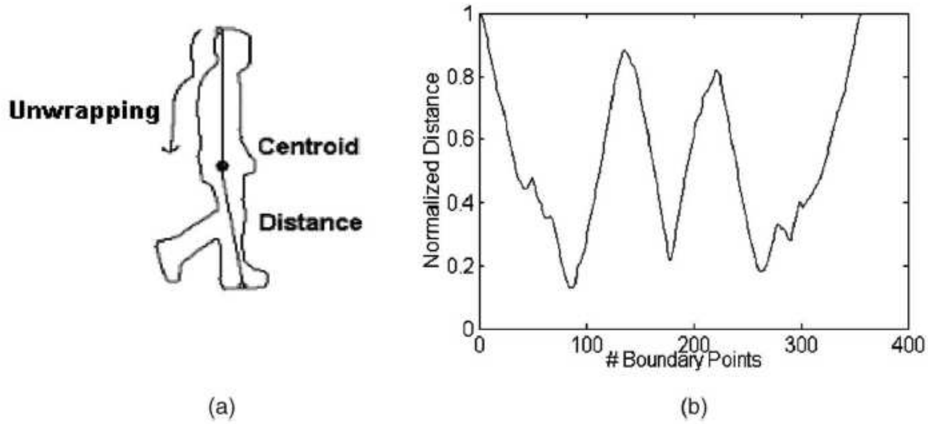

Figure 11: Silhouette representation (a) boundary extraction (b) 1D distance signal [82].

sets of features and classification techniques [80]. Benabdelkader et. al. [81] used stride length and cadence as features extracted from 17 subjects' silhouettes walking in outdoor environment for 30 meters on a straight line at fixed speed to achieve EER of 11% using linear regression for classification. Wang et. al. [82] utilized the silhouette structure evolution over time time to characterize gait, by calculating the silhouette center and obtaining its contour they converted the 2D silhouette into 1D signal by calculating the distance between the centroid and every pixel on the contour see figure 11. Principal component analysis (PCA) were used for dimensionality reduction of normalized distance signals using normalized euclidean distance (NED) as similarity measure and nearest neighbor classifier with respect to class exemplars (ENN) classification approach, achieved EER of 20%, 13%, and 9% for 20 subjects were filmed at 0, 45, and 90 degrees view respectively.

Cunado et. al. [83] extracted the gait feature from legs by modeling leg as two joined pendula see figure 12. The change of inclination angle of the thigh and shin was transformed to frequency domain using Fourier transform. They obtained 40% classification rate using k-nearest neighbors (KNN) for magnitude spectra of the frequency components. By using magnitude spectra togother with phase spectra classification rate was improved to be 90%.

In [84] nine dynamic and static features were collected from body silhouettes. The discrete cosine transform (DCT) was applied on the extracted feature vectors to de-correlate them. Encoded version of the transformed signal was fed to generalized regression neural network (GRNN), the recognition rate was 100%, 93.33% and 92.5% for 20, 30, and 40 subjects respectively. Singh and Jain [85] used dynamic body features to characterize human gait. They used hand and foot's toe, heel points to draw two triangles among hand, toe and heel, two intersecting points are calculated and angles at these points to form four feature vectors extracted from each frame of

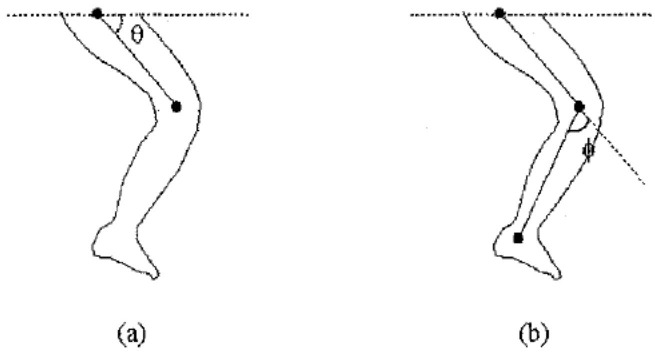

Figure 12: (a)Hip and (b) knee rotation angles [83].

the video sequence as shown in figure 13 . Using video sequences of 17 subjects taken at 90 degrees view, they achieved average classification rate of 78% based on angles mean values and intersecting points.

The most relative work to to ours was done by He and Le [18], in which temporal leg angles was used as gait features for four walking styles, slow, fast, incline and walking with a ball, on a running machine, they achieved wide range of correct recognition rate (CRR) for the different walk styles using nearest neighbor (NN) and ENN classification techniques. The best result for 9 subjects were in worst case 74,91% using NN for the shin parameters alone in fast walk and best case 100% using NN for merging thigh and shin parameters in ball walk. Running the test over the whole CMU database 96.39 % was achieved for fast-walk. Jensen et. al [86] used time of flight camera to analyze gait , i their work step and stride length, speed ,cadence and angles of joints were extracted as gait features. They used model fitting technique to extract the joint angles.

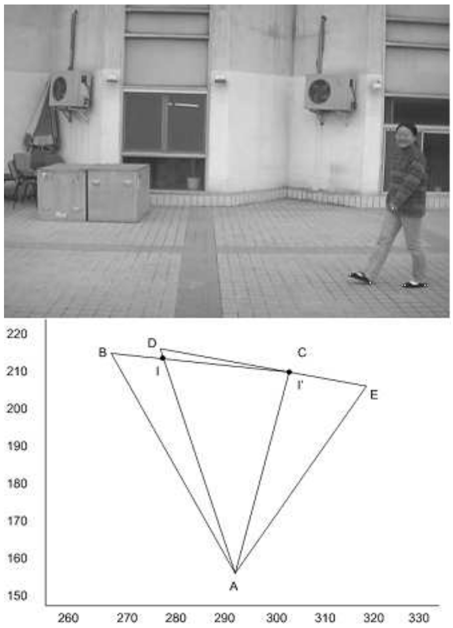

Figure 13: Dot points on subject's selected features (top), triangles created on selected features (down) [85].

4 Technology

4.1 Time of flight sensor

Imaging using ToF cameras is a new technique, which acquires intensity images and distance images at high frame rates [87, 88]. The distance image is a range measure for each pixel in the intensity image see figure 14. The main advantage of ToF) technology over stereoscopy and other 3D imaging technologies is that it can acquire 3D point cloud from a single point of view. This type of sensors introduce also some errors in the range measurements. The other limitations include low resolution up to few kilo pixels and limited range of measurements [89].

4.1.1 ToF measurement principle

In stereo vision systems two cameras are required to take two images of the same object as shown in figure 15, by finding the corresponding pixel in the other image to calculate the position by the triangulation principle [90]. The main disadvantages of stereo vision that it requires high processing power to find the corresponding pixels and they may not be found correctly due to illumination condition . In ToF technique the sensor sends infra-red light towards the scene and, the reflected light from objects, returns on the sensor array of the camera where a phase detector delivers at the pixel i a sinusoidal signal [91]. The range can simply be measured by calculating the round trip time of the light as

$$L = \frac{1}{2} c\, T_d \tag{4.1}$$

where $c = 3 \times 10^{-8} m/sec$ is the speed of light and T_d is the light's round trip time. The other method of ToF imaging uses modulated infrared light and the distance measurement depends on the phase difference of the light. The amplitude $A(i)$ is proportional to the object reflectivity and the phase $\phi(i)$ is proportional to the distance $d(i)$ of the object to the camera.

$$I(i) = a(i) e^{j\varphi(i)} \tag{4.2}$$

Figure 14: Example of ToF camera image: (a) intensity image (b) range image.

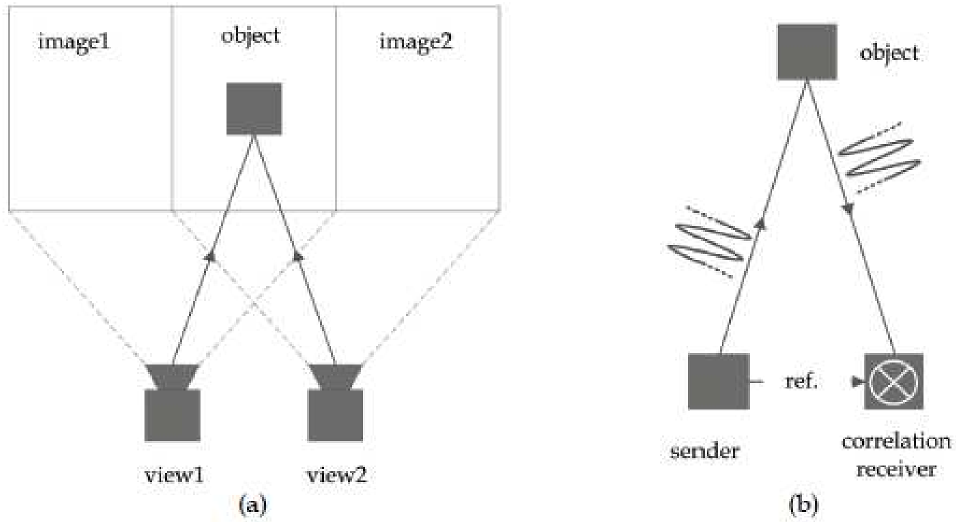

Figure 15: Working principle (a) stereo vision systems (b) ToF vision systems [92].

$$\varphi(i) = 4f\pi d(i)/c. \tag{4.3}$$

where $c = 3 \times 10^8 m/sec$ is the speed of light and f stands for the modulation frequency. The reflected signal is sampled four times, at 1/4 period phase shift see figure 16, due to the quantum nature of light time windows of Δt are used to sample the reflected light signal, where Δt is half of the modulation wavelength out of the four measurements the phase shift φ, offset and the Amplitude A can be measured as

$$\varphi = \left(\frac{c(\tau_0) - c(\tau_2)}{c(\tau_1) - c(\tau_3)} \right), \tag{4.4}$$

$$B = \frac{c(\tau_0) + c(\tau_1) + c(\tau_2) + c(\tau_3)}{4}, \tag{4.5}$$

$$A = \frac{\sqrt[2]{(c(\tau_0) - c(\tau_2))^2 + (c(\tau_1) - c(\tau_3))^2}}{2}, \tag{4.6}$$

$$L = \frac{\lambda_{mod}}{2} . \frac{\varphi}{2\pi}. \tag{4.7}$$

4.1.2 Non-ambiguity range

Tof range imagers are susceptible to a phenomena called ambiguity or back-folding, which occurs due to the periodic nature of the modulating signal [94]. The non-ambiguity range can be calculated from equation 4.7, where $\varphi = 2\pi$ and for example $f = 15\,\text{MHz}$, the non-ambiguity range is 10 meters. Since the phase detector is limited to measure phase rage of $0 - 2\pi$ so it can correctly measure the distance of object at distance D, the objects at points farther than this range D are folded back to this range as shown in figure 17.

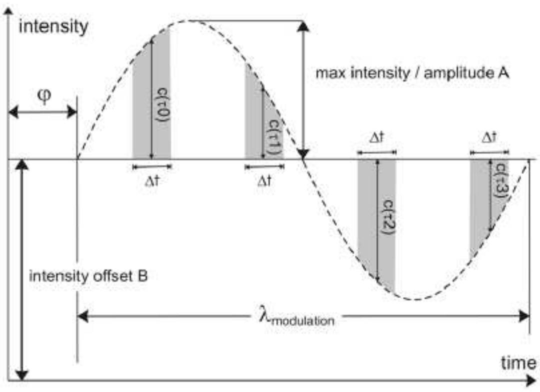

Figure 16: Phase shift distance measurement principle [93] .

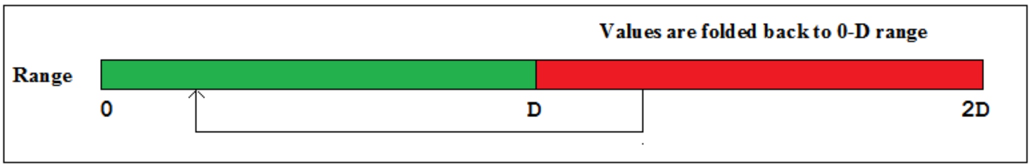

Figure 17: Illustration of non-ambiguity range.

4.1.3 Range measurement errors

The ToF sensors like any other electronic devices are susceptible to systematic and non-systematic errors, these errors influences the attained range measurements by the sensors. Many experimental tests [89, 93, 95, 96, 97] were performed on different models of ToF sensors to evaluate their performance and calibrate the introduced errors.

Temperature dependent errors

A general problem in semiconductor technology is that the materials are highly affected by changes in the temperature. An increased temperature causes a higher rate of thermally generated electrons, which adds to the system's noise. The systems showed sensitivity to the internally generated heat and by the surrounding temperature.

Intensity dependent errors

Tests showed that objects placed at the same distance with different intensities were perceived to be at different distances, the range of pixels with relatively small intensity is measured incorrectly. When objects are too close to the sensor, becomes saturated and the range readings are invalid.

Integration time related error

Integration time (IT) is the time period that the pixels are given to collect the light, the acquired frame rate is inversely proportional to the integration time. By selecting different IT's, different

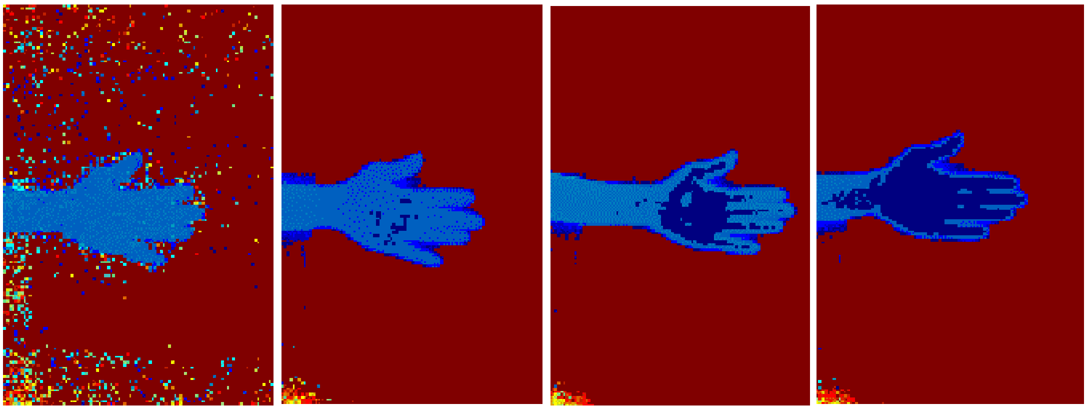

Figure 18: The figure shows the effects of IT, images taken using different IT's has different artefatcs, noisy image at (a), the saturation artefact increases as the integration time increased (a)IT=0.5 ms (b)IT=5 ms (c) IT=10ms (d) IT = 20ms.

range measurements were observed for the same scene. Using high IT sensor becomes saturated so the range readings are invalid, see figure 18.

Scattering errors

Light scattering due to multipath reflections of light from the scene which distorts the reflected signal. The second type of scattering occurs inside the camera between the lens, the optical filter and the sensor, the second case has larger effect because the scattered signal does not only affect the correspondent pixels but also some of the other pixels in the image [97].

Motion related error.

This type of error occurs when there are moving objects in the scene. Since the main range measurement depends on the sampling of the reflected light from the object, objects motion may not allow the camera to capture the four required samples needed to calculate the range of the intended pixel correctly see figure 19 , as some of the taken samples belong to other pixel in the scene [98].

4.1.4 SR-4000 sensor

In this work we used Swiss ranger SR-4000 CW10 see figure 20 sensor by Mesa technologies [24]. The SR4000 is an optical imaging system housed in an anodized aluminum enclosure. The camera operates with 24 LED emitting infra-red in the 850nm range, it modulates the illumination light emitting diodes (LED) at modulation frequency of 15MHz. Range measurements are obtained at each pixel using the phase shift principle, with non-ambiguity range of 10 meters. Figure 21 shows the measurement regions of the camera, in normal operation an absolute accuracy of less than 1cm is achievable. The camera has USB port for data acquisition and supplied with software library for C and Matlab. The specification of the sensor are shown in table 3 .

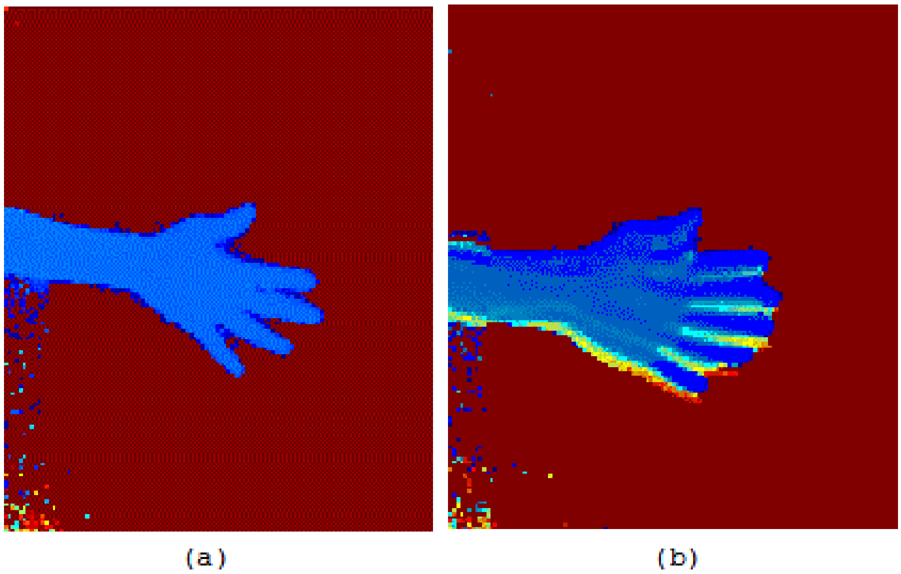

Figure 19: Images taken from distance of 1 meter (a) Static hand (b) up and down hand in motion .

Figure 20: SR-4000 ToF sensor

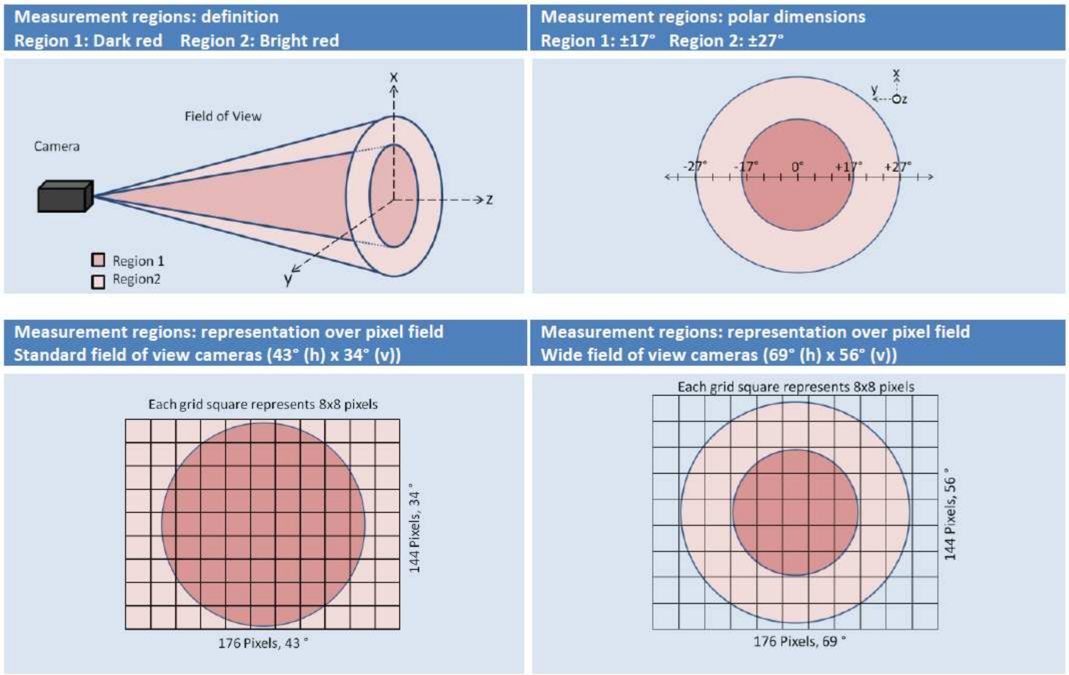

Figure 21: Definition of measurement regions

Item	Specifications
Pixel array size [-]	176 (h) × 144 (v)
Field of view [°]	43.6 (h) × 34.6 (v)
Pixel pitch [μm]	40
Illumination wavelength with standard settings [nm]	850
Working range with standard settings [m]	0.3 - 5.0
Maximum frame rate [fps]	54
Dimensions [mm]	65 × 65 × 68
Weight [g]	470

Table 3: SR-4000 sensor specifications

4.2 Prototype development tools

We used Matlab to develop the prototype for this project. Matlab is widely used tool because of its simplicity and wide range of tool boxes, image processing, signal processing and statistics tool boxes, these tools are easy to use and Mathworks website provides good support for these tools, which adds to the advantages of using Matlab. Another good reason for selecting Matlab is the availability of many already developed codes and function relative to image processing, using just codes saves a lot of time which can be wasted in coding all the prototype from scratch. As hardware platform for image acquisition and further processing and analysis we used laptop with the following specs:

- Processor: Pentium Dual-Core CPU 2.0 GHz
- RAM: 4 GB
- Operating system : Windows 7 professional (32-bit)

5 Feature extraction

5.1 Overview

Subjects Image sequence is acquired using the ToF camera, while walking parallel to the camera. Followed by segmentation to extract the subjects body silhouette, morphological operations is applied to reduce background noise and holes in the extracted human silhouette images. Next, each of the enhanced human silhouettes is divided into six body segments based on human anatomical knowledge [99]. Ellipse fitting is applied to each of the six segments, the orientation of each of the ellipses is used to calculate the orientation of each of the lower body parts for further analysis.

5.2 Video Segmentation

Video segmentation is the process of partitioning a video spatially or temporally. It is an integral part of many video analysis and coding problems, including video indexing and retrieval, video coding, motion analysis and surveillance. In order to perform gait analysis of a person from image sequence the subject needs to be extracted from the background of the video sequence. Image segmentation is used to separate foreground objects like people, from the background of the image sequence. Thresholding is the simplest image segmentation technique, each pixel in the original image is compared to a specified threshold if the pixel's intensity value is greater than the threshold value it is set as foreground pixel with value 1 if not its set to zero as background pixel producing a binary image, see figure 22. In some complex images the operation can be iterated using two thresholds, in this case threshold works like band pass filtering.

$$out(i,j) = \begin{cases} 1, \text{ if } & I(i,j) > th \\ 0, & otherwise \end{cases} \tag{5.1}$$

To apply thresholding to separate out the foreground of an image on the basis of pixel intensity, there should be clear distinction between foreground and background elements in the image. Histograms can be used to find the proper threshold values[100], where peaks correspond to foreground objects are used to determine the threshold values. If the image's histogram shows no clear peaks, then, thresholding can not produce a acceptable segmentation. In this case, another technique should be used.

5.3 Morphological operations

Mathematical morphology is shape based technique for processing of digital images [101]. Morphological operations are used to simplify image data preserving their main shape characteristics and eliminating irrelevant details. Morphological operations have two inputs the original image and structuring element to be applied to the input image, creating an output image of the same size. In a morphological operation, the value of each pixel in the output image is based on a com-

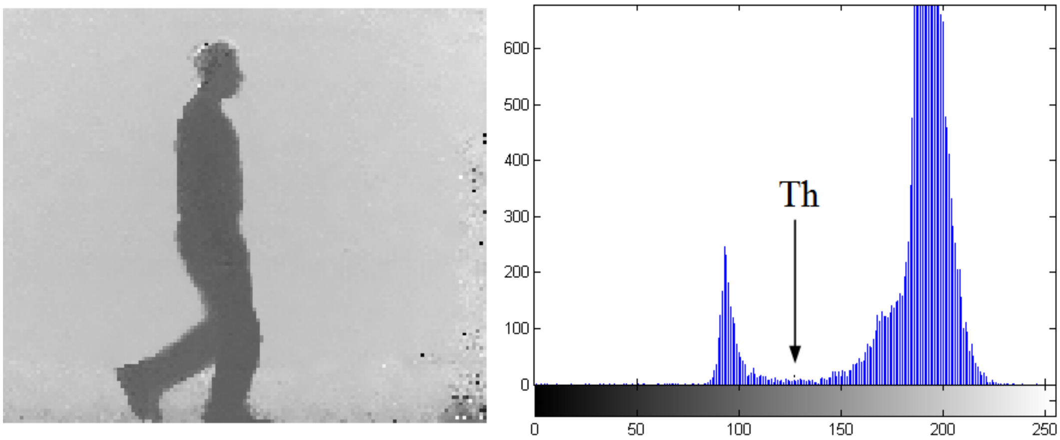

Figure 22: Segmentation result, (left)Original depth image (right) image's histogram .

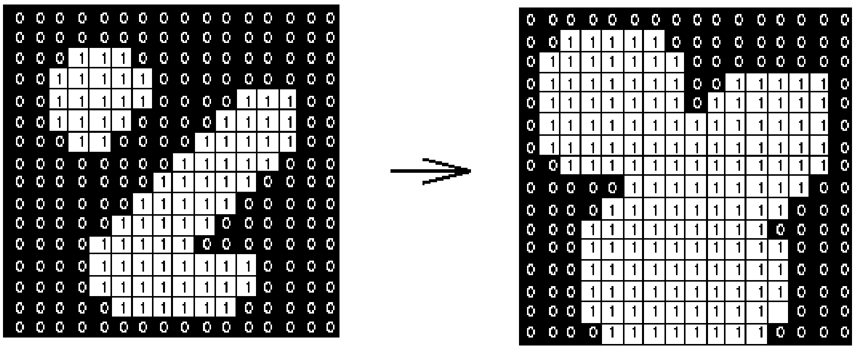

Figure 23: Effect of dilation using a 3×3 square structuring element.

parison of the corresponding pixel in the input image with its neighbors. The shape and size of the structuring element constructs a morphological operation that is sensitive to specific shapes in the input image. The most basic morphological operations are dilation and erosion.

5.3.1 Dilation

Dilation is a morphological operation which enlarges the foreground region by a factor each iteration by adding pixels to the boundaries of objects in an image.It works by placing the structuring element on top of the input image so that the origin of the structuring element is a foreground input pixel coordinates. If at least one pixel in the structuring element coincides with a foreground pixel in the image underneath, then the input pixel is set to the foreground value. If all the corresponding pixels in the image are background, however, the input pixel is left at the background value, see figure 23.

5.3.2 Erosion

Erosion is a morphological operation which reduces the foreground region by a factor each iteration by removing pixels from object boundaries. It works by placing the structuring element on top of the input image so that the origin of the structuring element is a foreground input pixel coordinates. For each of the pixel in the structuring element, the corresponding pixel in the image underneath is a foreground pixel, then the input pixel is left as it is. If any of the corresponding pixels in the image are background, however, the input pixel is also set to background value, see figure 24.

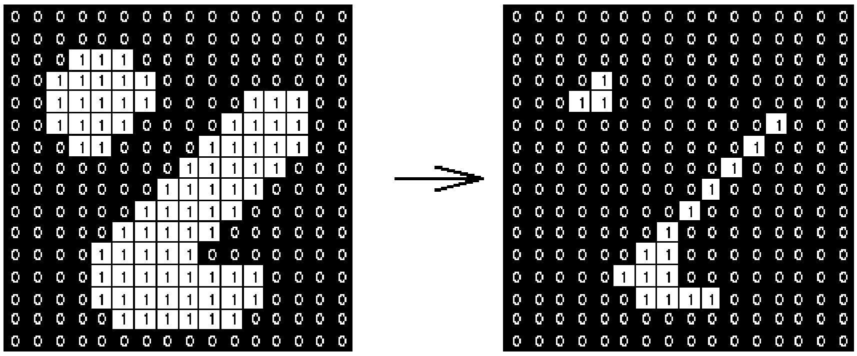

Figure 24: Effect of erosion using a 3×3 square structuring element.

5.3.3 Connected component labeling

Connected components labeling scans an image and classifies its pixels into components according to their connectivity. All the pixels in a connected component have the same intensity values and are in some way connected with each other. Once all groups have been determined, each pixel is labeled with a value similar to the component it was assigned to. The image is scanned from top to bottom and from left to right two times in order to identify connected pixel regions, see figure 25.

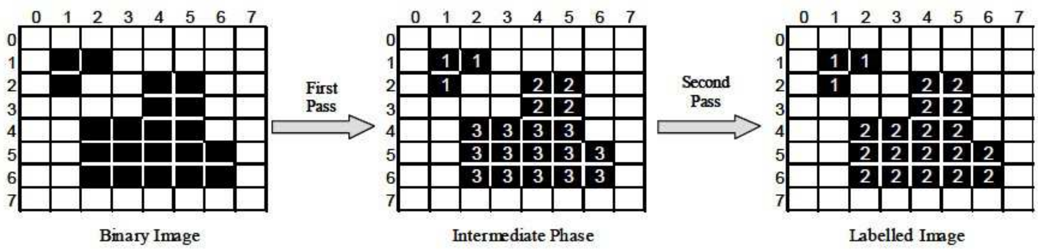

Figure 25: Connected component labeling example.

We use opening and closing followed by connected body labeling to enhance the segmented object. Opening is erosion followed by dilation, it used to filter out noise. Closing is dilation followed by erosion, it is used to close holes. the result of morphological operations is shown in figure 26

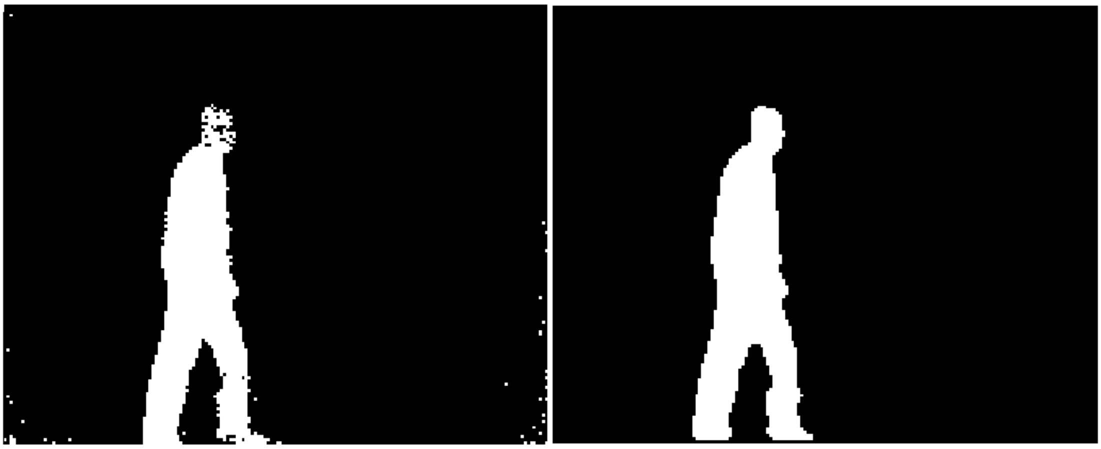

Figure 26: Morphological filtering, (left) thresholded image (right) morphologically filtered image.

5.4 Ellipse fitting

Having extracted body silhouette, the subject body were segmented into six parts [99]. First, the centroid of the subject is determined by calculating the center of mass of the silhouette. The area above the centroid is considered as the upper body head, neck and torso. The area below the centroid is considered as the lower body legs and feet. Next, one third of the upper body is divided as the head and neck. The remaining two thirds of the upper body are classified as the torso. The lower body is divided into two portions thighs and shin. Fitting an ellipse to each of the six body parts and finding the center of mass , orientation , and major axis length we characterized these body parts see figure 27. Evolution of the these parameters for the video sequence describes the human gait characteristics in time.

Figure 27: (a) 6 Body parts (b) Ellipse fitting model .

5.5 Leg tracking

Gait analysis requires reliable tracking of moving human body segments. As the human body's segmented into six parts, we need to track the lower limbs in each frame to construct meaningful output of the measured angles in the following step. To Track the body parts along the image sequence we utilize the depth information acquired at each moment, we calculate the mean range values of the segment. The segment with higher mean range values belong to the farthest leg from the camera and vice versa, in figure 28 a sample sequenceof images with tracking results are shown.

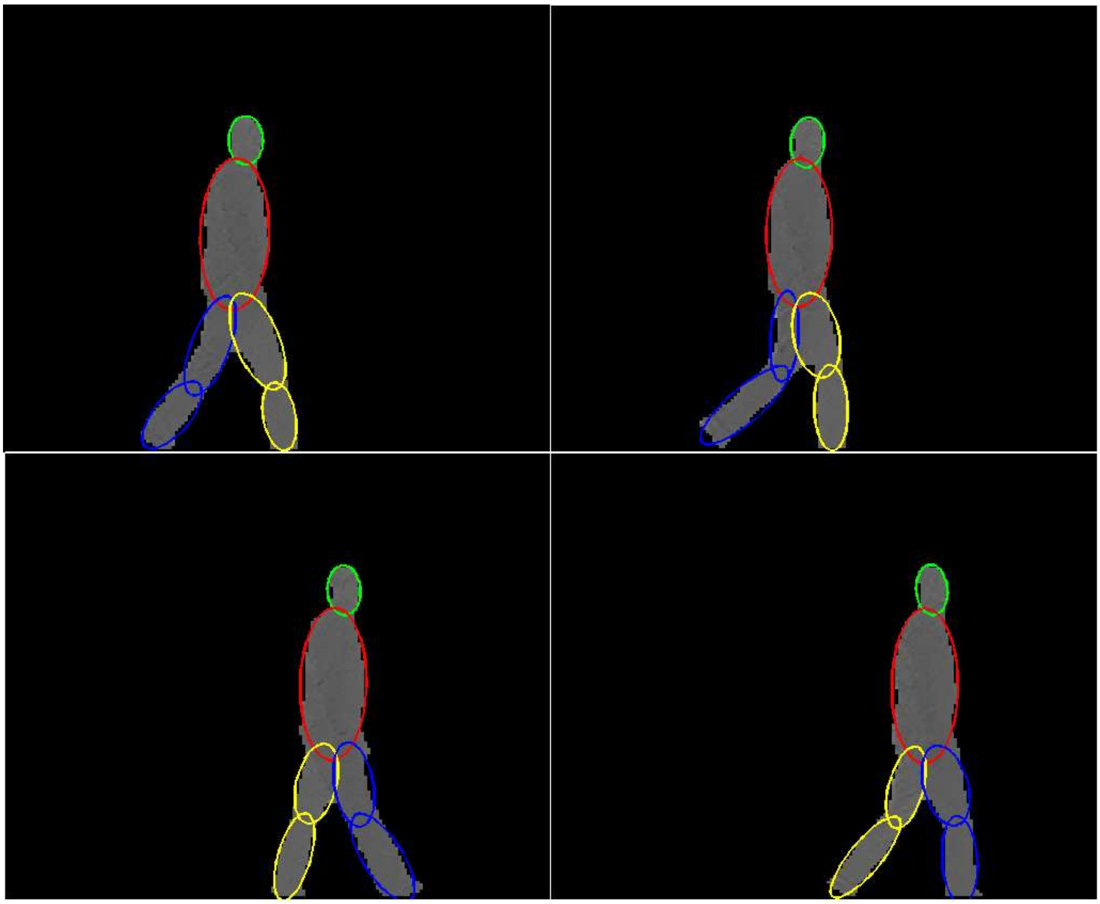

Figure 28: Tracking of legs, blue ellipses for the leg closer to the camera.

5.6 Leg angles calculation

Human body is modeled as rigid segments connected by joints. The simplest model as 2D stick [102], as in figure (29-a). to extract the gait signatures we will mainly extract the thigh and shin angles from each frame of the video sequence to characterize the gait cycle. In this final step we extract the angles based on the data extracted data from ellipse fitting to the body segments. The fitted ellipse parameters orientation, major axis length and centroid will be used

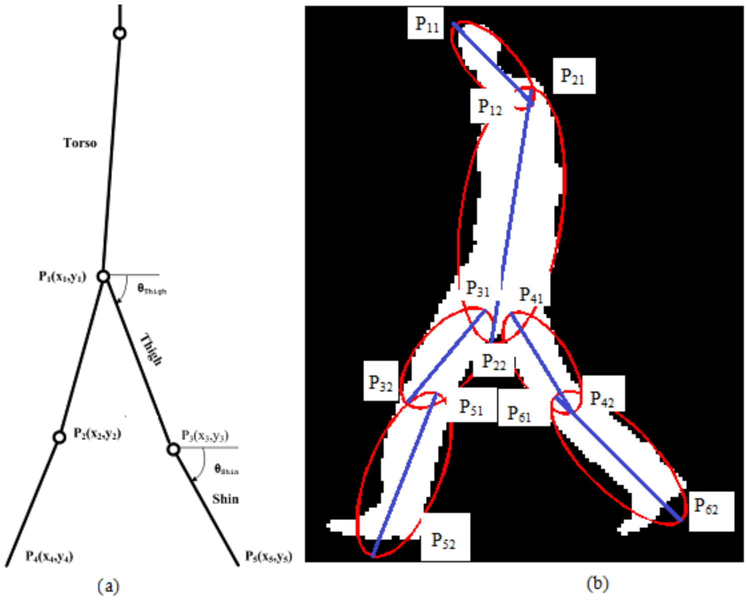

Figure 29: Illustration of joint locations, (a) 2D stick figure, (b) sample frame.

to approximately calculate the start and end points coordinates for each of the body segments, such that each segment will be defined by two points in two dimensional space ((p_{i1},p_{i2}) using equations (5.2, 5.3, 5.4, 5.5) as shown in figure (29-b).

$$x_1 = x_0 + l_{major} * \cos(phi) \tag{5.2}$$

$$x_2 = x_0 - l_{major} * \cos(phi) \tag{5.3}$$

$$y_1 = y_0 + l_{major} * \sin(phi) \tag{5.4}$$

$$y_2 = y_0 - l_{major} * \sin(phi) \tag{5.5}$$

To calculate the angles of the leg segments, we reduce the impact of the non-precise fitting of the ellipses to the body segments, we assume the location of the joints as the average location of the start point of one of the segments and the end point of the segment connected by the joint. The hip and knee joint's location are calculated by the equation set (5.6, 5.7, 5.8), as shown in figure 30

$$p_1 = \frac{p_{22} + p_{31} + p_{41}}{3} \tag{5.6}$$

$$p_2 = \frac{p_{32} + p_{51}}{2} \tag{5.7}$$

$$p_3 = \frac{p_{42} + p_{61}}{2} \tag{5.8}$$

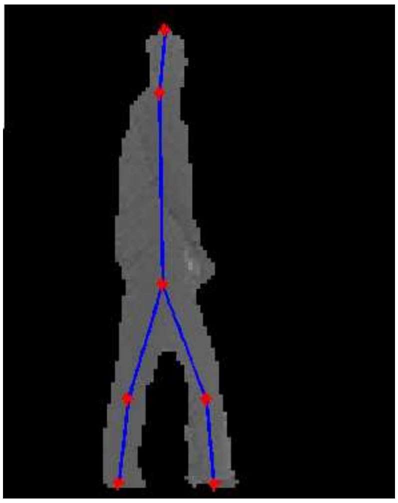

Figure 30: Joint location calculation.

The extracted features for each of the segments were calculated by equation 5.9. We calculate the inclination angle of thigh and shin for each of the subject's legs to characterize the gait by the evolution of these angles in time at each image of the video sequence. Since the gait is quasi-periodic movement we extract a single gait cycle from each video sequence.

$$\theta = \arctan\frac{y_2 - y_1}{x_2 - x_1} \tag{5.9}$$

The extracted feature are filtered using a local median filter to filter out the outliers. The outliers can be due to losing track of the legs, or bad ellipse fitting, in figure 31 plots for 5 different gait cycle for one subject before and after filtering.

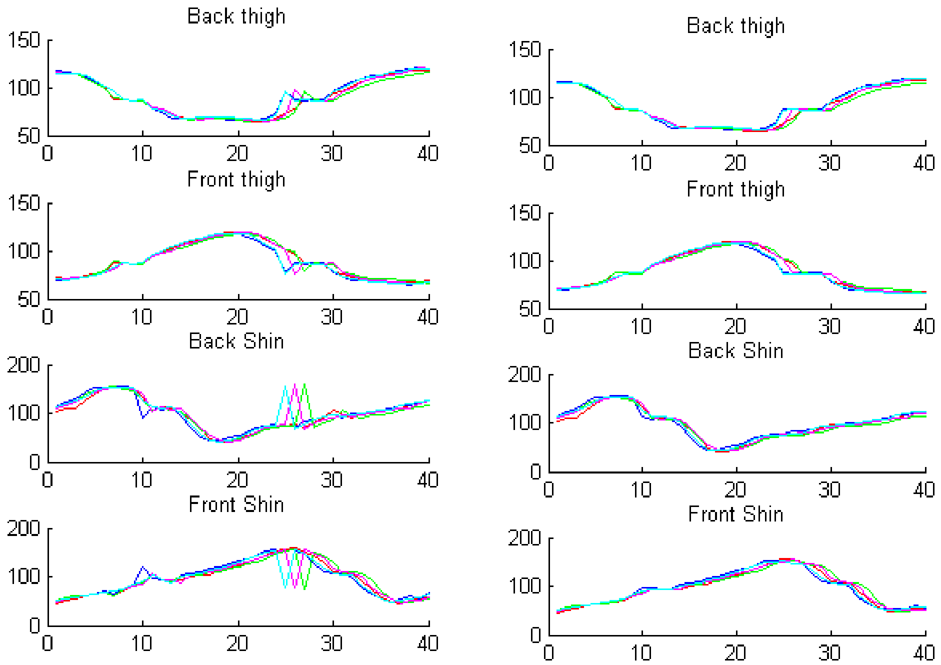

Figure 31: Extracted data for 5 different walking cycles,left: original data, right:filtered data.

6 Experiment

In order to verify the usefulness of the proposed system, we performed an individual gait identification experiment. In this chapter we will go through the different issues related to our experiment.

6.1 Experiment setup

The subject's motion was filmed from the side by means of a ToF camera at 30 frames/sec, while the subject was walking on a track in front of the camera as shown in figure 32. Due to the camera's narrow field of view, the length of the filmable track was limited to about 3 meters. Therefore the subjects were asked to walk back and forth 10 times in a track longer than the field of view's width. We used this longer track to allow recording the subject in full motion. To reduce the noise in the distance, the camera was calibrated such that the image starts from the walking track in order to eliminate the reflection from the floor. The camera was put on tripod at 70 cm height from the floor and was tilted up about 5 degrees, as recommended by the camera manufacturer, see figure 33.

6.2 Experiment execution

The experiment was carried out on a solid surface in the lab. The subjects were asked to walk a fixed track in front of the camera. This fixed track allow the participants to walk for 1.5 to 2 gait cycles depending on the participants gait characteristics, and because some of the participants may not start precisely at the marker where the view field of the camera starts. Each participant walks the track at least 10 times to extract one full gait cycle from each pass in front of the camera. The experiment procedure by the participant can be summarized in three steps to be repeated 10 times in average.

1. Walk the track.
2. Turn around.
3. Walk the track back.

6.3 Environment

The experiment to be held in the lab on a solid floor. The walking track is marked on the floor such that the distance between the camera and the track is about half the distance from the sensor and the wall of the lab with no any other objects in the scene.

6.4 Volunteers

The experiment was done in Gjøvik University College. An invitation was sent to the students at the faculty to participate in the experiment, and 30 participants volunteered to participate in this experiment. They were of different age and height groups. The average age for the volunteers

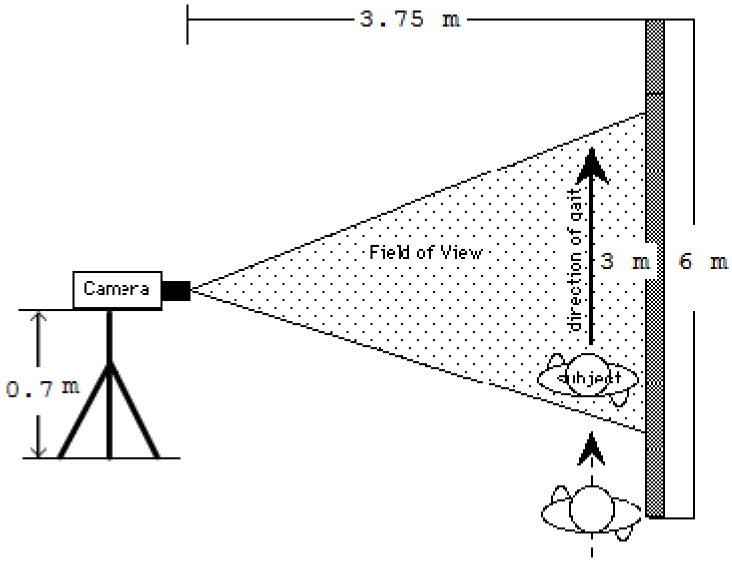

Figure 32: Experiment's walking path

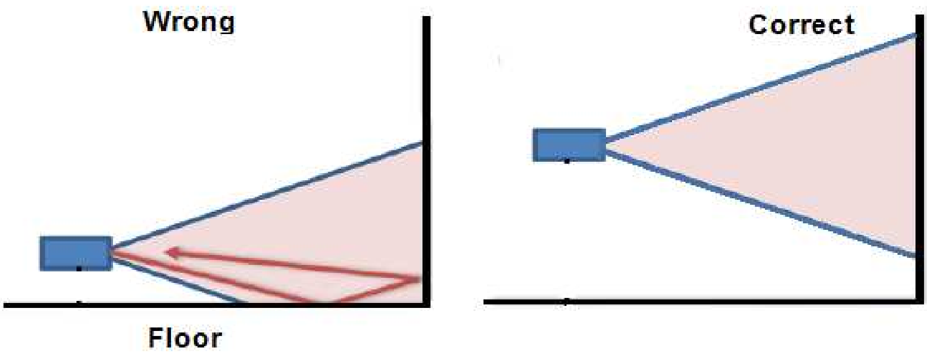

Figure 33: Positioning of the camera to avoid reflection.

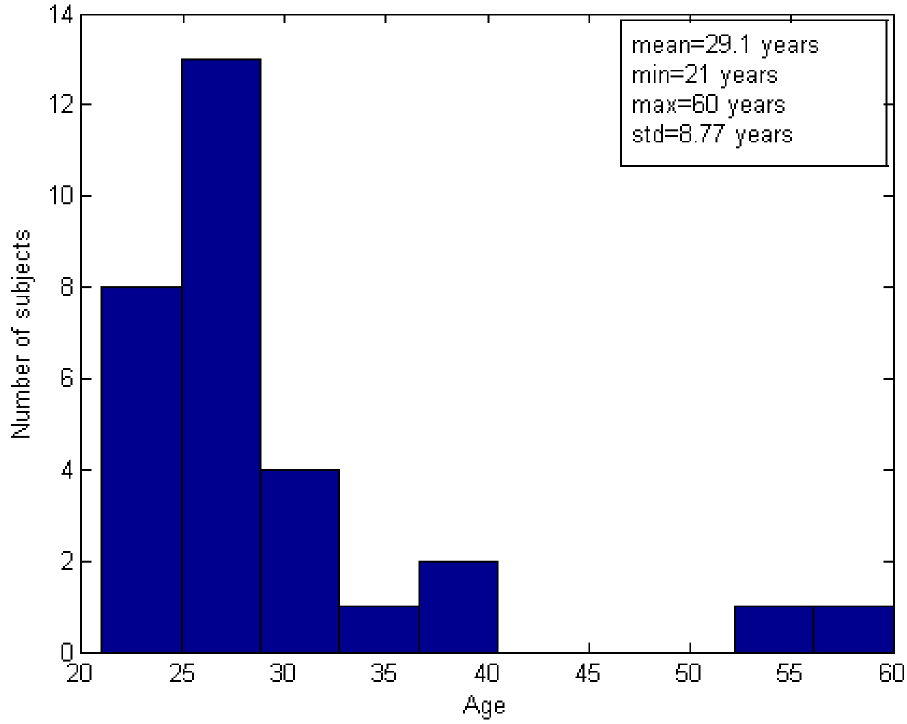

Figure 34: Age distribution of the participants.

was 29.1 years, see the graph in figure 34, the average height was 176.9 cm, see the graph in figure 35. The participants were asked to wear the same type of shoes through the two sessions. The experiment is composed of two sessions, during which we collected the data for the 30 subjects over a month, time gap between the two session varies from subject to subject, for example for subjects it was one week and for others about a month.

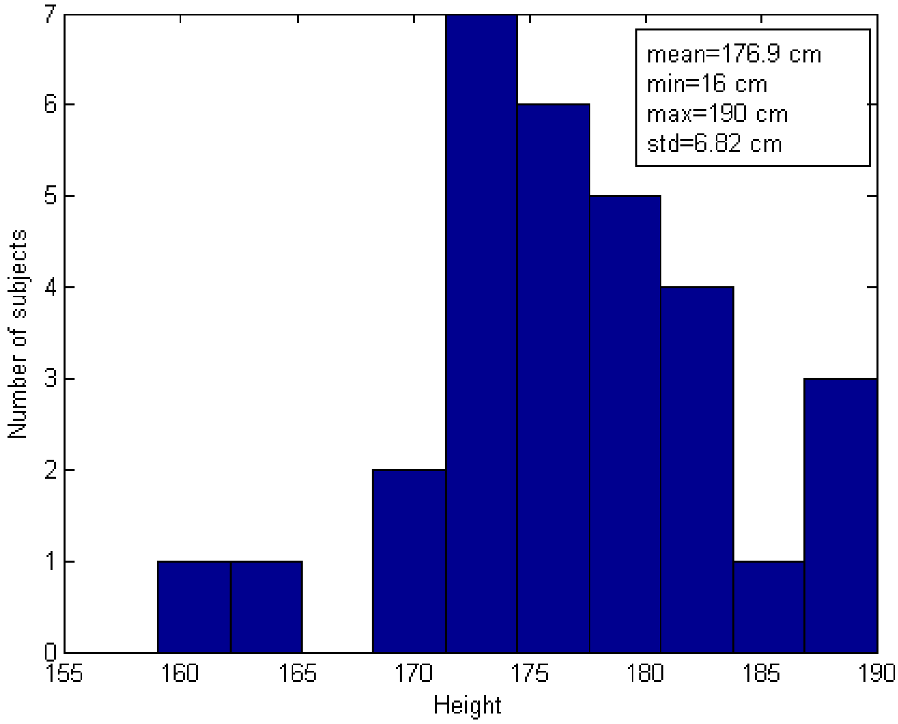

Figure 35: Height distribution of the participants.

7 Analysis and results

This chapter presents a description of analysis techniques and the achieved results in the context of a novel gait recognition system based on ToF sensor. First sketches how a template is extracted. Section two presents the similarity measure which comparison methods have been applied. Third section covers the topic of comparison tables that gives a clear overview of how the comparison scores are matched against each other. The fourth sections illustrate practical examples gait scores. In addition it also exemplify how False Match Rate (FMR), False None-Match Rate (FNMR), Equal Error Rate (EER) and Decision Trade-off (DET) curves are computed. The last sections describes the achieved results from our experiment.

7.1 Creation of templates

Before we are capable of calculating the overall (distance or similarity) score we must first create templates for each gait cycle as we saw in Chapter 5. The template is a processed and stored; representing the distinguishing characteristics of a subject's gait. It is stored during the enrollment and is later used for comparison. Due to variations in the way biometric sample is captured, two templates from the same biometric will never be identical. This is the origin of the probabilistic nature of biometrics, as the comparison process can only give a decision condense and not an absolute assurance (refer to chapter 2). There are numerous ways to process and analyze the gait raw data which the video analysis produces. The main phases involved of creating a gait template are as follows:

- Noise reduction: Removes/reduces the noise from the gait signal using median/ average filters .
- Cycle detection: An important phase is to detect where a cycle starts and ends. There are different ways to split up a signal into periodic cycles. In this project we used manual split from peak to peak.
- Template Creation: After the cycles have been identified one needs to create a template for enrollment that shall be compared against another test-template. One simple way of doing this is to normalize all the steps to have equal length and take the mean or median from these steps. Another possibility is to not normalize the cycle length but use Dynamic Time Warping (DTW).

7.2 Similarity score calculation

When all templates are created from each subject, an algorithm will take the features from one stored reference template, along with the features extracted from the rest of the templates, and compare them to generate similarity scores, which indicates the likelihood that both are from the same person. The output similarity score may come in a variety of forms, as from zero to hundred (similarity score), unbounded, or the closer the score to zero is , the more similar the templates are (dissimilarity score).

Dynamic time warping (DTW):

Because the gait cycles are not equal in length we used DTW which measures the similarity between unequal sequences. We used the same approach used by [103] which is based on the classical approach of DTW [104]. The major difference between the approaches is that in [104] they made no distinction between costs related to insertions, deletions and substitutions.

7.3 Comparison table

An example of how the output looks like for gait scores is shown in listing 7.1. The first column indicates the index/comparison number. Column two and three are the files (or templates) that are compared against each other. As can be seen, the filename has a special convention, see appendix B. Column 4 indicates the score of the two files compared against each other and the last column tells whether it is a genuine or an impostor attempt.

```
001  <s1_02_01_01.txt> <s1_02_01_01.txt> [02.54]  (G)
002  <s1_02_01_02.txt> <s2_02_04_02.txt> [04.33]  (G)
003  <s1_02_01_01.txt> <s2_02_01_01.txt> [05.26]  (G)
...  <s1_02_01_01.txt> <s2_03_01_01.txt> [15.33]  (I)
...  <s1_02_01_01.txt> <s1_03_01_01.txt> [27.37]  (I)
...  <s1_02_01_01.txt> <s1_01_01_02.txt> [60.13]  (I)
```

Listing 7.1: Sample of the scores as it is stored

When comparing templates with each other, it will not be useful to compare a template against itself as it will always give an perfect score of 100 % match. The templates that are matched against all the other samples produced by the same subject are indicated as genuine attempts and the templates matched against others are indicated as the impostor or fraudulent attempts. In Table 4 is a small sample of a comparison score table for comparing templates from the same Database ($DB_X = DB_X$).

	P_1S_1	P_1S_2	...	P_1S_k	P_2S_1	P_2S_2	...	P_nS_k
P_1S_1	-	-	...	-	-	-	...	-
P_1S_2	G	-	...	-	-	-	...	-
...	⋮	⋮	⋮	...	...	⋮	⋮	⋮
P_1S_k	G	I	...	-	-	-	...	...
P_2S_1	I	I	...	I	-	-	...	...
P_2S_2	I	I	...	I	G	-	...	-
⋮	⋮	⋮	⋮	...	...	⋮	⋮	⋮
P_nS_k	I	I	I	I	I	I	...	-

Table 4: Comparison scores from the same Gait-ID and same database ($DB_x = DB_x$). G = [genuine], I = [impostor], P = [subject-ID] and S = [session-ID].

Assume having N subjects and S gait cycles per subject. When comparing two templates the total number of genuine attempts will be.

$$G_{tot} = \frac{S * (S - 1) * N}{2} \tag{7.1}$$

while total number of impostor attempts will be:

$$I_{tot} = \frac{S^2 * (N-1) * N}{2} \tag{7.2}$$

Each algorithm is tested by performing the following comparisons:

Genuine recognition attempts: The template of each gait cycle is compared to the remaining templates of the same subject, but avoiding symmetric matches (i.e. if the template of gait cycle j is matched against the template of gait cycle k, template k is not matched against j);

Impostor recognition attempts: The template of each gait cycle is compared to the remaining templates of the other subjects,avoiding symmetric matches.

As we mentioned earlier, each participant walked in two different sessions, and each session was downloaded as a separate file to the PC. Each of these files contained the data of five assessed gait data, each again separated by leg types, i.e. front shin, back shin, front thigh and back thigh. In each file the data representing more than one gait cycle was manually aligned and cut such that one cycle started at a minimum and ended at a minimum value. This was applied for all files. So the data from each collected file was split into 4 other files (for each leg type). Using the above method the originally 30*5 = 150 collected files were split into 150*4 = 600 files, where each file contained the data of exactly one gait cycle in each leg type. Each file was labeled in such a way that participant, session number (1 or 2) and type of leg (front shin, back shin, front thigh, back thigh) were identifiable from the file name. Each file contained one column, representing the feature vector. The length of this feature vector varied indicates the length of walk gait cycle and was variating from one participant to another. For the second session, 20 out of the 30 volunteers participated. This means that the performance evaluation over a certain time interval will only consist with 20 volunteers.

7.4 Calculation of FMR, FMNR, EER and DET-curve

After scores have been calculated for gait templates, we can now initiate the creation of Decision Error Trade-off (DET) curve for each score set. The DET curve shows the trade-off between the rate of false non-match (FMNR) and chance of a false match (FMR). A curve from a good system will be located near the bottom of the graph (high verification rate for most false match rates see Figure 36-left). The following describes how the different error rates and curves have been calculated. Pseudo codes that will be used here:

Creation of List :

- List(gen) all genuine scores
- List(imp) all impostor scores
- List(all) both genuine and impostor scores

Calculation of false match rate (FMR):

The False Match Rate is calculated as shown in the Pseudo code (Listing 7.2). By having a nested loop, we first count the number of scores which are smaller than all the different thresholds in the list of both genuine and impostor. The reason why we increment the smaller is because the data files are of similarity measures and not dissimilarity.

```
        for each ( score s in List —{ a l l } )
{
threshold = s ;
for each ( score s in List —{ gen })
{
genuine_score = gs ;
i f ( genuine score < threshold )
genuine_counter++;
}
fmr = genuine_counter / total_number_of _genuines ;
}
```

Listing 7.2: Pseudocode for calculating false match rate (FMR)

Calculation of false none match rate (FNMR):

There are two changes here from the previous FMR calculation, see listing 7.3. The first change is that now we look for if the chosen impostor score is greater than the threshold. And the other change is that we now divide by the total number of impostors for finding the FNMR value. Two small changes, but very important.

```
        for each ( score s in List —{ a l l }
{
threshold = s ; \\ The similarity threshold
for each ( score s in List —{ imp }
{
impostor_score = is ;
if ( genuine score > threshold )
impostor_counter++;
}
fnmr = impostor_counter / total_number _of_impostors ;
}
```

Listing 7.3: Pseudocode for calculating False non match rate (FNMR)

When the threshold, FMR and FNMR values are calculated, then they are outputted to a file as shown in Listing 7.4. The three columns indicate the threshold value and their following FMR and FMNR.

```
Threshold     FMR          FNMR
 0.205     0.0031453    0.0135271
 0.6863    0.0000000    0.4762859
 1.1379    0.0000000    0.9679359
 0.6204    0.0000000    0.3700735
 0.3299    0.0000000    0.0612892
 0.0884    0.5516748    0.0001670
 0.1132    0.2814693    0.0006680
 0.1357    0.1219002    0.0016700
 0.1126    0.2874137    0.0006680
 0.1354    0.1233640    0.0016700
 0.1524    0.0579226    0.0041750
 0.1347    0.1270555    0.0015030
```

Listing 7.4: Output file for creating DET- curve

Calculation of equal error rate (EER) and decision error trade-off (DET)

The value indicates that the proportion of false match is equal to the proportion of false non-match. The lower the equal error rate value, the higher the accuracy of the biometric system. A sample graph would look like Figure (36-right) and as you can see from the graph, the EER occurs where the two lines cross. To calculate the DET of a biometric system, each corresponding FMR and FNMR point is plotted on a logarithmic scale or scale from 0 - 1 (36- left). The EER is then found by extending a 45-degree line from the point of origin (0,0). This line crosses the DET is the EER.

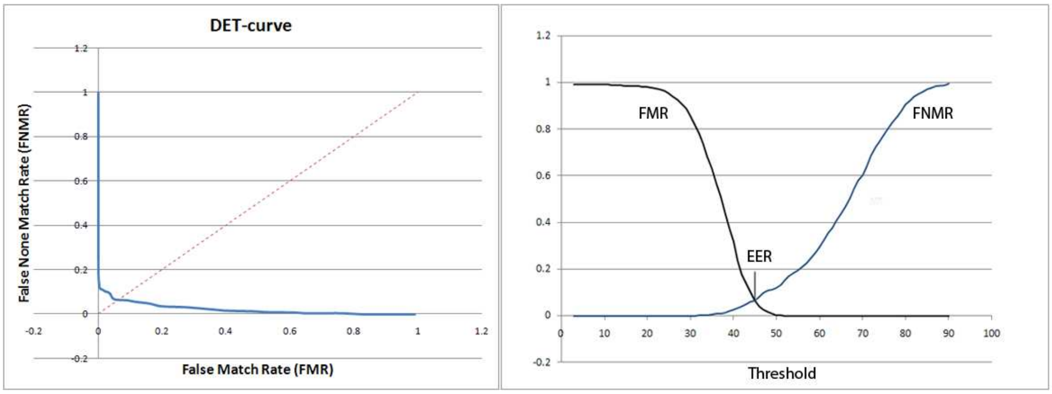

Figure 36: Calculating EER from FMR / FNMR intersection.

7.5 Results

Several performance evaluations were performed, figures 37, 38 and 39 show the results obtained using the shins, thighs and all features. Table 5shows the performance of the first session with 30 subjects (second column) and with the subset of 20 users (third column) who participated at the second session also. The first column indicates which template and test input were applied for performance testing. Notice that if we apply all the four types of leg as feature vector for one subject, we gain an better EER than when applying each separately. This is due to the fact that more information is stored for one subject. Another thing to notice here is that the thigh

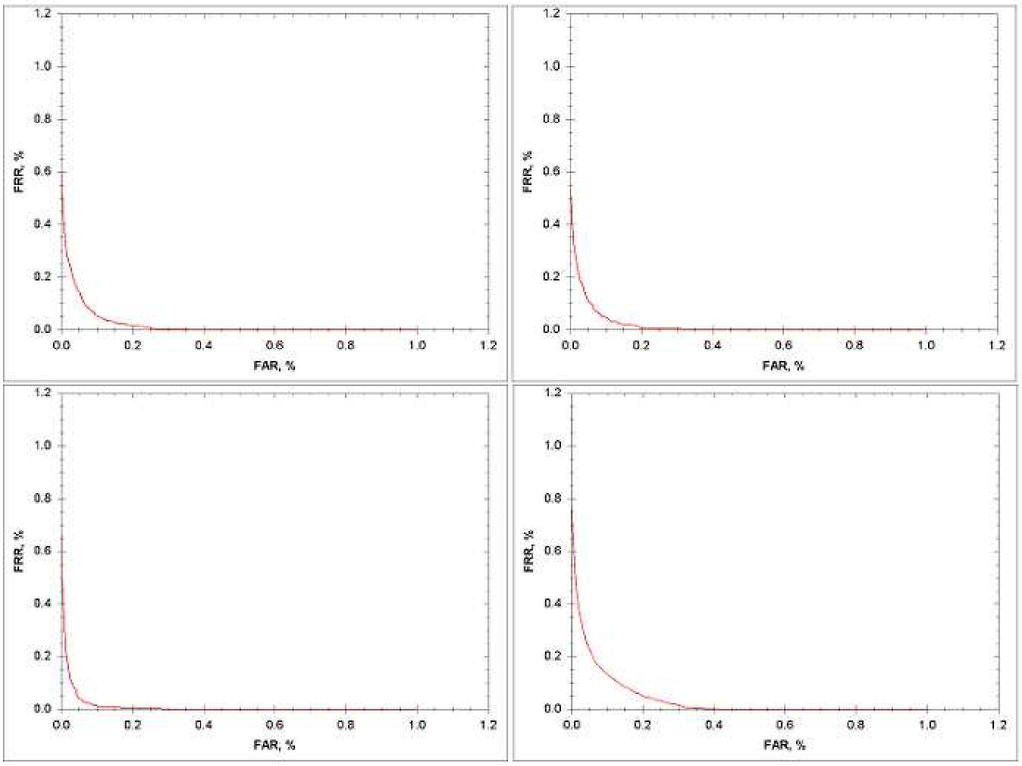

Figure 37: Shin Thigh DET curves, top-left: first session 30 participants, top-right: first session 20 participants, bottom-left: second session 20 participants, bottom-right: over-time 20 participants.

feature vector has better EER compared to shin. Since only a subset of users participated at the second session the EER has changed but not significantly.

Template/Test	30 Participants	20 Participants
Back thigh	8.42	7.48
Front thigh	7.39	6.62
Two thighs	5.50	5.03
Back shin	12.31	11.16
Front shin	11.32	10.24
Two shins	7.77	7.09
All features	4.63	4.08

Table 5: EER performance results in % on the collected dataset.

The performances for the second session are shown in Table 6. We observe a significant change of the performance and the reason is that the users are more used to the walking the second session and more comfortable with the experiment.

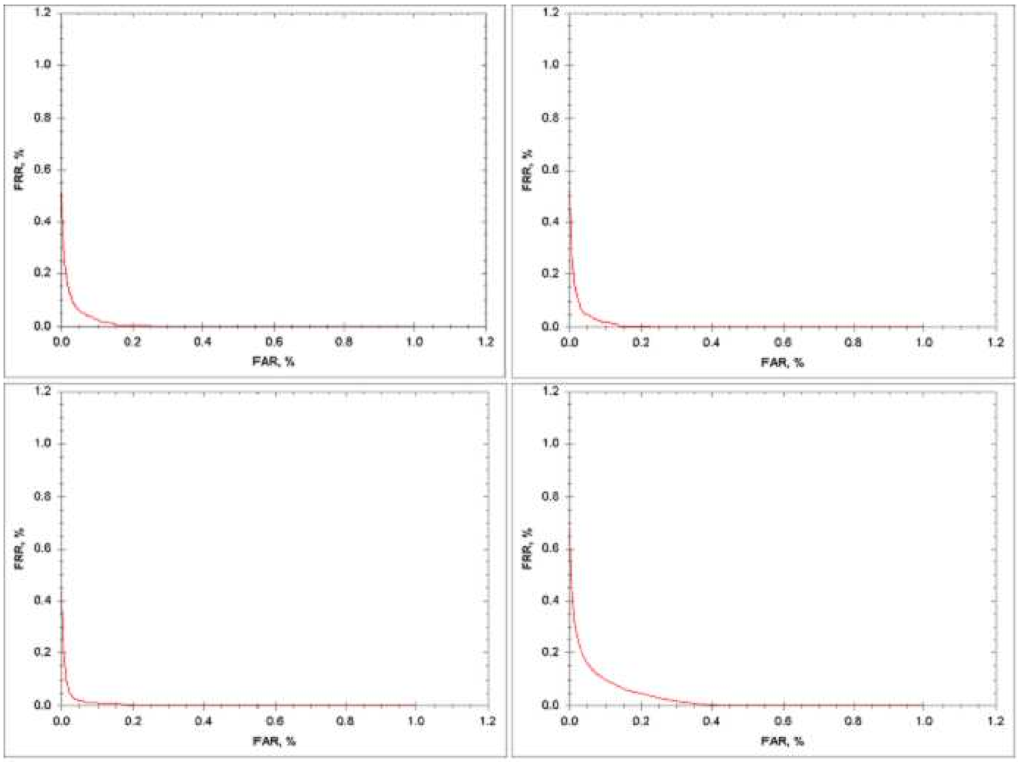

Figure 38: Thigh Thigh DET curves, top-left: first session 30 participants, top-right: first session 20 participants, bottom-left: second session 20 participants, bottom-right: over-time 20 participants.

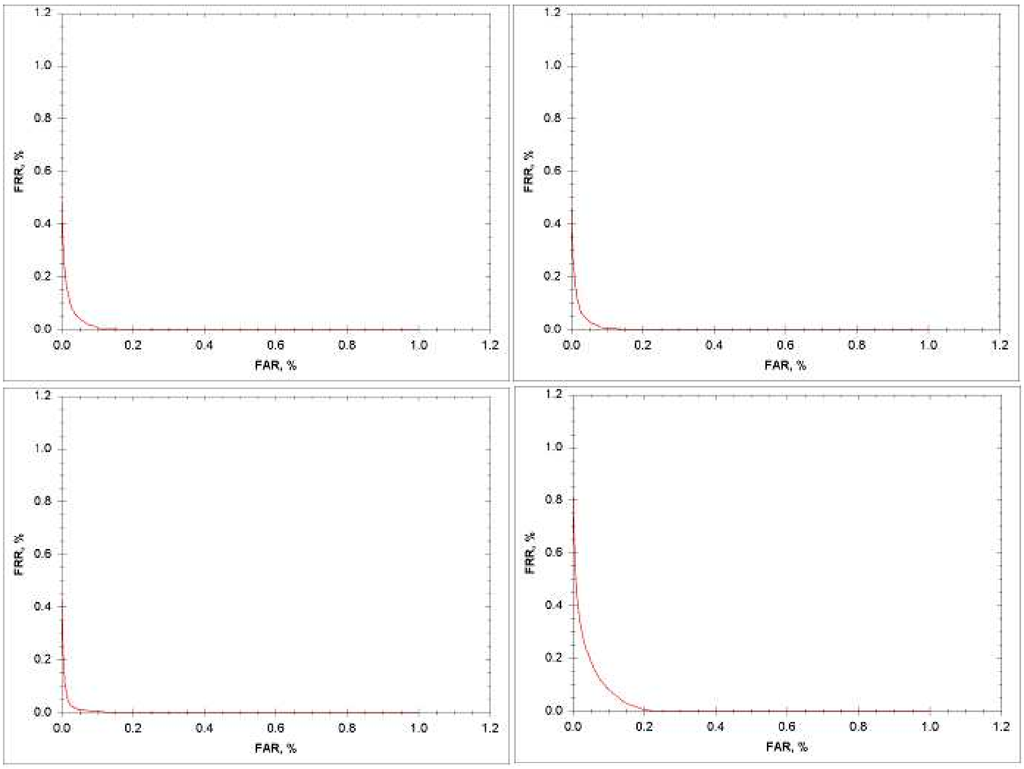

Figure 39: All features Thigh DET curves, top-left: first session 30 participants, top-right: first session 20 participants, bottom-left: second session 20 participants, bottom-right: over-time 20 participants.

Template/Test	Session 1	Session 2
Back thigh	7.48	4.72
Front thigh	6.62	6.02
Two thighs	5.03	3.19
Back shin	11.16	6.28
Front shin	10.24	9.41
Two shins	7.09	4.46
All features	4.08	2.62

Table 6: EER performance results in % on the collected dataset (20 users).

An interesting performance analysis is to investigate the change between the two session as can be seen in table 7. We are analyzing what will happen if we apply the first sessions data as training set and the sessions data as test set. What we observed here is that the change over time becomes worse. Different shoe-wearing, clothes wearing have impact on the achieved performance. The achieved results for a single session outperform the reported results of EER 5% by Wang et. al. [80] using wearable sensors and also the results achieved using machine vision by Wang et. al. [105] in which EER of 8% was at the same view angle.

Template/Test	Session 1	Session 2	Session 1+Session 2
Two thighs	5.03	3.19	9.91
Two shins	7.09	4.46	11.61
All features	4.09	2.48	9.25

Table 7: EER performance results in % where Session 1 data as template reference and session 2 data as test input (20 users).

8 Conclusion

This project aimed to investigate the usability of ToF sensors for gait recognition. The range information provided by the ToF are precise enough and showed a very interesting segmentation results. We also used the range information for tracking of different legs which also saved computation power for other tracking algorithms. The main problems we faced using the ToF camera : 1) the camera is sensitive to multiple reflections, 2) the reflectivity of the objects in the scene, 3) motion blur when there is moving object in the scene, 4) the limited view field of the camera. To reduce the impact of these factors we had to develop the special camera setup as mentioned in section (6.1). The overall performance of the camera was promising and we think in the near future new models of the camera with better resolution and lower cost will developed. This type of technology can have numerous applications in robotics, automotive and surveillance field and machine vision. To find which gait features can be used to characterize a person, we reviewed the literature and found that there is a lot of previous studies with different sets of features. As the gait is the “manner of walking” we used the leg segments inclination as a feature set to recognize people. Employing human anatomical knowledge for segmenting body parts, ellipse fitting technique was effective in extracting the needed features, followed by post processing step to reduce the impact of non-precise fitting of the ellipses. The extracted features were robust and followed a representative pattern of the motion of each of the leg segments. Testing the accuracy of the achieved inclination angles is out of the scope of this project as we are mainly concerned with the evolution of these angles in time. When analyzing the data we could already visually see that gait cycles were detectable for each subject and are clearly dissimilar from others’. The experiment was performed over two different days (sessions) where each of the subjects (first session 30 subjects, second session 20 subjects) walked a predefined track within the camera field of view. Using DTW the best equal error rate obtained was 2.66 % for a single session where the with change over time we retrieve an equal error rate of about 9.25%. Although the achieved over time results are not as good as those of individual sessions they are promising as first step toward a better performance in the future. As per our knowledge this this is the first gait recognition system based on ToF technology, we have submitted a papaer titled "Gait Recognition using Time-of-Flight Sensor" based on this work to BIOSIG 2011 [106].

Future work may include the development of more robust segmentation technique as the main hypothesis was that a single subject is present in the scene which is not practical in actual surveillance scenarios. For the feature extraction part the system should be able to extract the feature from different view angles. For the recognition part more work with multiple session over multiple days, and more cycles per person to evaluate the stability over time under different covariant factors.

Bibliography

[1] Mosby. 2008. *Mosby's Medical Dictionary*. Elsevier Science Inc.

[2] Waki, K., Iwam, T., Matsunaga, T., Shimada, Y., & Obinata, G. nov. 2009. Gait estimation using foot-pressure sensors. In *Micro-NanoMechatronics and Human Science, 2009. MHS 2009. International Symposium on*, 62 –67.

[3] Suutala, J., Fujinami, K., & Röning, J. 2008. Gaussian process person identifier based on simple floor sensors. In *Proceedings of the 3rd European Conference on Smart Sensing and Context*, EuroSSC '08, 55–68, Berlin, Heidelberg. Springer-Verlag.

[4] Qian, G., Zhang, J., & Kidane, A. sept. 2010. People identification using floor pressure sensing and analysis. *Sensors Journal, IEEE*, 10(9), 1447 –1460.

[5] Moeslund, T. B., Hilton, A., & Krüger, V. November 2006. A survey of advances in vision-based human motion capture and analysis. *Comput. Vis. Image Underst.*, 104, 90–126.

[6] Rodriguez-Silva, D. A., Gil-Castineira, F., Gonzalez-Castano, F. J., Duro, R. J., Lopez-Pena, F., & Vales-Alonso, J. 2008. Human motion tracking and gait analysis: a brief review of current sensing systems and integration with intelligent environments. In *IEEE Conference on Virtual Environments, Human-Computer Interfaces and Measurement Systems, 2008. VECIMS 2008.*, 166–171.

[7] Faugeras, O. & Robert, L. 1996. What can two images tell us about a third one? *International Journal of Computer Vision*, 18, 5–19.

[8] Macellari, V. 1983. Costel: a computer peripheral remote sensing device for 3-dimensional monitoring of human motion. *Medical and Biological Engineering and Computing*, 21, 311–318. 10.1007/BF02478500.

[9] Kirk, A., O'Brien, J., & Forsyth, D. 2005. Skeletal parameter estimation from optical motion capture data. In *Computer Vision and Pattern Recognition, 2005. CVPR 2005. IEEE Computer Society Conference on*, volume 2, 782 – 788 vol. 2.

[10] Stancic, I., Borojevic, D., & Supuk, T. September 2009. Development and testing of a device for human kinematics measurement. *WTOS*, 8, 1083–1092.

[11] Ferrigno, G. & Pedotti, A. nov. 1985. Elite: A digital dedicated hardware system for movement analysis via real-time tv signal processing. *Biomedical Engineering, IEEE Transactions on*, BME-32(11), 943 –950.

[12] Josefsson, T., Nordh, E., & Eriksson, P.-O. 1996. A flexible high-precision video system for digital recording of motor acts through lightweight reflex markers. *Computer Methods and Programs in Biomedicine*, 49(2), 119 – 129.

[13] Kakadiaris, I. & Metaxas, D. jun. 1996. Model-based estimation of 3d human motion with occlusion based on active multi-viewpoint selection. 81 –87.

[14] Wang, L., Ning, H., Tan, T., & Hu, W. 2004. Fusion of static and dynamic body biometrics for gait recognition. 14(2), 149–158.

[15] Bouchrika, I. & Nixon, M. S. March 2007. Model-based feature extraction for gait analysis and recognition. In *Mirage: Computer Vision ? Computer Graphics Collaboration Techniques and Applications*, volume 4418, 150–160.

[16] Niyogi, S. & Adelson, E. jun 1994. Analyzing and recognizing walking figures in xyt. In *Proceedings of IEEE Computer Society Conference ,on Computer Vision and Pattern Recognition CVPR '94.*, 469 –474.

[17] Wang, L., Hu, W., & Tan, T. 2003. Recent developments in human motion analysis. Pattern Recognition, vol. 36,no. 3, pp. 586-601.

[18] He, W. & Li, P. 2010. Gait recognition using the temporal information of leg angles. In *3rd IEEE International Conference on Computer Science and Information Technology (ICCSIT),*, volume 5, 78 –83.

[19] Nguyen, A. V. & Lee, E.-J. 2009. Real-time human recognition by their walk. In *Proceedings of First Asian Conference on Intelligent Information and Database Systems ACIIDS 2009*, 386–391.

[20] MURRAY, M. P., DROUGHT, A. B., & KORY, R. C. 1964. Walking patterns of normal men. *J Bone Joint Surg Am*, 46(2), 335–360.

[21] Cutting, J., . K. L. 1977. Recognizing friends by their walk: Gait perception without familiarity cues. *Bull. Psychon. Soc.*, Vol. 9, pp. 353–356.

[22] Kozlowski, L. T. & Cutting, J. E. 1977. Recognizing the sex of a walker from a dynamic point-light display. *Perception Psychophysics*, 21(6), 575–580.

[23] Johansson, G. 1973. Visual perception of biological motion and a model for its analysis. *Perception and Psychophysics*, 14, 201–211.

[24] Mesa. http://www.mesa-imaging.ch/.

[25] Jain, A. K., Ross, A., & Prabhakar, S. 2004. An introduction to biometric recognition. 14(1), 4–20.

[26] Bolle, R., Ratha, N., & Pankanti, S. 2005. Performance evaluation in 1 : 1 biometric engines. In *Advances in Biometric Person Authentication*, Li, S., Lai, J., Tan, T., Feng, G., & Wang, Y., eds, volume 3338 of *Lecture Notes in Computer Science*, 257–286. Springer Berlin - Heidelberg.

[27] Peterson, W., Birdsall, T., & Fox, W. 1954. The theory of signal detectability. *IRE Professional Group on Information Theory*, 4(4), 171–212.

[28] Galton, F. 1892. *Finger prints*. Macmillan and Co.

[29] Nixon, M. S., Tan, T. N., & Chellappa, R. 2005. *Human Identification based on Gait*. International Series on Biometrics. Springer.

[30] Lee, L. & Grimson, W. E. L. 2002. Gait analysis for recognition and classification. In *Proc. Fifth IEEE Int Automatic Face and Gesture Recognition Conf*, 148–155.

[31] Menant, J. C., Steele, J. R., Menz, H. B., Munro, B. J., & Lord, S. R. 2009. Effects of walking surfaces and footwear on temporo-spatial gait parameters in young and older people. *Gait & Posture*, 29(3), 392 – 397.

[32] Zhang, R., Vogler, C., & Metaxas, D. june 2004. Human gait recognition. In *Computer Vision and Pattern Recognition Workshop, 2004. CVPRW '04. Conference on*, 18.

[33] Yu, S., Tan, D., & Tan, T. 2006. A framework for evaluating the effect of view angle, clothing and carrying condition on gait recognition. In *Proceedings of the 18th International Conference on Pattern Recognition - Volume 04*, ICPR '06, 441–444, Washington, DC, USA. IEEE Computer Society.

[34] Chan, C. W. & Rudins, A. 1994. Foot biomechanics during walking and running. *Mayo Clinic proceedings Mayo Clinic*, 69(5), 448–461.

[35] Bolle, R. & Pankanti, S. 1998. *Biometrics, Personal Identification in Networked Society: Personal Identification in Networked Society*. Kluwer Academic Publishers, Norwell, MA, USA.

[36] Davis, R. B., Ounpuu, S., Tyburski, D., & Gage, J. R. 1991. A gait analysis data collection and reduction technique. *Human Movement Science*, 10(5), 575 – 587.

[37] Tanawongsuwan, R. & Bobick, A. 2001. Gait recognition from time-normalized joint-angle trajectories in the walking plane. In *Proceedings of the IEEE Computer Society Conference on Computer Vision and Pattern Recognition, 2001. CVPR 2001.*, volume 2, II–726 – II–731 vol.2.

[38] Bobick, A. F. & Johnson, A. Y. 2001. Gait recognition using static, activity-specific parameters. In *Proc. IEEE Computer Society Conf. Computer Vision and Pattern Recognition CVPR 2001*, volume 1.

[39] Veres, G. V., Nixon, M. S., Middleton, L., & Carter, J. N. 2005. Fusion of dynamic and static features for gait recognition over time. In *Proc. 8th Int Information Fusion Conf*, volume 2.

[40] Wang, L., Ning, H., Tan, T., & Hu, W. 2003. Fusion of static and dynamic body biometrics for gait recognition. In *Proc. Ninth IEEE Int Computer Vision Conf*, 1449–1454.

[41] Pratheepan, Y., Condell, J., & Prasad, G. sept. 2009. The use of dynamic and static characteristics of gait for individual identification. In *Machine Vision and Image Processing Conference, 2009. IMVIP '09. 13th International*, 111 –116.

[42] Stevenage, S. V., Nixon, M. S., & Vince, K. 1999. Visual analysis of gait as a cue to identity. *Applied Cognitive Psychology*, 13(6), 513–526.

[43] Micera, S., Carpaneto, J., Scoglio, A., Zaccone, F., Freschi, C., Guglielmelli, E., & Dario, P. 2004. On the analysis of knee biomechanics using a wearable biomechatronic device. In *Proc. IEEE/RSJ Int. Conf. Intelligent Robots and Systems (IROS 2004)*, volume 2, 1674–1679.

[44] Lindinger SJ, Soggl T, M. E. H. H. 2008. Control of speed during the double poling technique performed by elite cross-country skiers. In *Medicine & Science in Sports & Exercise: January 2009 - Volume 41 - Issue 1 - pp 210-220*.

[45] Kobashi, S., Kawano, K., Tsumori, Y., Yoshiya, S., & Hata, Y. 302009-april2 2009. Wearable joint kinematic monitoring system using inertial and magnetic sensors. In *IEEE Workshop on Robotic Intelligence in Informationally Structured Space (RIISS).*, 25 –29.

[46] Ascension. http://www.ascension-tech.com/.

[47] OHGI, Y. Mems sensor application for the motion analysis in sports science. *ABCM Symposium Series in Mechatronics - Vol. 2 - pp.501-508*.

[48] Fuller, J., Liu, L. J., Murphy, M. C., & Mannl, R. W. 1997. A comparison of lower-extremity skeletal kinematics measured using skin- and pin-mounted markers. *Human Movement Science*, 16(2-3), 219 – 242. 3-D Analysis of Human Movement - II.

[49] Maletsky, L. P., Sun, J., & Morton, N. A. 2007. Accuracy of an optical active-marker system to track the relative motion of rigid bodies. *Journal of Biomechanics*, 40(3), 682 – 685.

[50] engineering, B. http://www.btsbioengineering.com/ita/index.html.

[51] Qualisys. http://www.qualisys.com/.

[52] Coda. http://www.codamotion.com.

[53] Analysis, M. www.motionanalysis.com.

[54] Li, H., Tang, J., Wu, S., Zhang, Y., & Lin, S. 2010. Automatic detection and analysis of player action in moving background sports video sequences. 20(3), 351–364.

[55] Goffredo, M., Schmid, M., Conforto, S., Carli, M., Neri, A., & D'Alessio, T. January 2009. Markerless human motion analysis in gauss-laguerre transform domain: an application to sit-to-stand in young and elderly people. *Trans. Info. Tech. Biomed.*, 13, 207–216.

[56] Sundaresan, A. 2005. Markerless motion capture using multiple cameras. In *In Computer Vision for Interactive and Intelligent Environment*, 15–26.

[57] Zhu, Y., Dariush, B., & Fujimura, K. 2008. Controlled human pose estimation from depth image streams. In *Proc. IEEE Computer Society Conf. Computer Vision and Pattern Recognition Workshops CVPRW '08*, 1–8.

[58] TOF, W. http://en.wikipedia.org/wiki/time-of-flight.

[59] Rosenhahn, B., Schmaltz, C., Brox, T., Weickert, J., Cremers, D., & Seidel, H.-P. 2008. Markerless motion capture of man-machine interaction. In *Computer Vision and Pattern Recognition, 2008. CVPR 2008. IEEE Conference on*, 1 –8.

[60] Murai, A., Yamane, K., & Nakamura, Y. 2009. Characterization of motor skill based on musculoskeletal model. In *Proc. Annual Int. Conf. of the IEEE Engineering in Medicine and Biology Society EMBC 2009*, 6542–6545.

[61] Paradiso, J., Abler, C., Hsiao, K.-y., & Reynolds, M. 1997. The magic carpet: physical sensing for immersive environments. In *CHI '97 extended abstracts on Human factors in computing systems: looking to the future*, CHI EA '97, 277–278, New York, NY, USA. ACM.

[62] Fernstroem, M. & Griffith, N. 1998. Litefoot - auditory display of footwork. University of Glasgow, U.K. British Computer Society, British Computer Society.

[63] McElligott, L., Dillon, M., Leydon, K., Richardson, B., Fernström, M., & Paradiso, J. 2002. Forse fields - force sensors for interactive environments. In *UbiComp 2002: Ubiquitous Computing*, Borriello, G. & Holmquist, L., eds, volume 2498 of *Lecture Notes in Computer Science*, 321–328. Springer Berlin / Heidelberg.

[64] Middleton, L., Buss, A., Bazin, A., & Nixon, M. oct. 2005. A floor sensor system for gait recognition. In *Fourth IEEE Workshop on Automatic Identification Advanced Technologies, 2005.*, 171 – 176.

[65] Orr, R. J. & Abowd, G. D. 2000. The smart floor: a mechanism for natural user identification and tracking. In *CHI '00 extended abstracts on Human factors in computing systems*, CHI EA '00, 275–276, New York, NY, USA. ACM.

[66] Qian, G., Zhang, J., & Kidané, A. 2008. People identification using gait via floor pressure sensing and analysis. In *Proceedings of the 3rd European Conference on Smart Sensing and Context*, EuroSSC '08, 83–98, Berlin, Heidelberg. Springer-Verlag.

[67] Sung, M., Marci, C., & Pentland, A. 2005. Wearable feedback systems for rehabilitation. *Journal of NeuroEngineering and Rehabilitation*, 2(1), 17.

[68] Heikki J. Ailisto, Mikko Lindholm, J. M. E. V. & Makela, S.-M. 2005. Identifying people from gait pattern with accelerometers. *Proc. SPIE ; doi:10.1117-12.603331*, Vol. 5779, pp. 7–14.

[69] Gafurov, D., Snekkenes, E., & Buvarp, T. 2006. Robustness of biometric gait authentication against impersonation attack. In *On the Move to Meaningful Internet Systems 2006: OTM 2006 Workshops*, Meersman, R., Tari, Z., & Herrero, P., eds, volume 4277 of *Lecture Notes in Computer Science*, 479–488. Springer Berlin / Heidelberg.

[70] Gafurov, D., Helkala, K., & Soendrol, T. april 2006. Gait recognition using acceleration from mems. In *Availability, Reliability and Security, 2006. ARES 2006. The First International Conference on*, 6 pp.

[71] Gafurov, D., Helkala, K., & Søndrol, T. 2006. Biometric gait authentication using accelerometer sensor. *Journal of Computers*, VOL. 1, No. 7.

[72] Rong, L., Jianzhong, Z., Ming, L., & Xiangfeng, H. May 2007. A wearable acceleration sensor system for gait recognition. In *Industrial Electronics and Applications, 2007. ICIEA 2007. 2nd IEEE Conference on*, 2654 –2659.

[73] Derawi, M. O., Nickel, C., Bours, P., & Busch, C. 2010. Unobtrusive user-authentication on mobile phones using biometric gait recognition. In *Proceedings of the 2010 Sixth International Conference on Intelligent Information Hiding and Multimedia Signal Processing*, IIH-MSP '10, 306–311, Washington, DC, USA. IEEE Computer Society.

[74] Nickel, C., Busch, C., Rangarajan, S., & Mobius, M. march 2011. Using hidden markov models for accelerometer-based biometric gait recognition. In *IEEE 7th International Colloquium on Signal Processing and its Applications (CSPA), 2011*, 58 –63.

[75] Sprager, S. & Zazula, D. 2009. Gait identification using cumulants of accelerometer data. In *Proceedings of the 2nd WSEAS International Conference on Sensors, and Signals and Visualization, Imaging and Simulation and Materials Science*, SENSIG'09-VIS'09-MATERIALS'09, 94–99, Stevens Point, Wisconsin, USA. World Scientific and Engineering Academy and Society (WSEAS).

[76] Hu, W., Tan, T., Wang, L., & Maybank, S. 2004. A survey on visual surveillance of object motion and behaviors. *IEEE–J–SMCC*, 34(3), 334–352.

[77] Larsen, P. K., Simonsen, E. B., & Lynnerup, N. 2008. Gait analysis in forensic medicine. *Journal of Forensic Sciences*, 53(5), 1149–1153.

[78] Geradts, Z. J., Merlijn, M., de Groot, G., & Bijhold, J. 2002. Use of gait parameters of persons in video surveillance systems. volume 4709, 16–24. SPIE.

[79] Kumar Neelesh, Kunju Nissan, K. A. S. B. S. 2010. Active marker based kinematic and spatio-temporal gait measurement system using labview vision. *JSIR*, Vol.69(08), 600–605.

[80] Wang, X., Li, Y., & Qiao, F. july 2010. Gait authentication based on multi-criterion model of acceleration features. In *Modelling, Identification and Control (ICMIC), The 2010 International Conference on*, 664 –669.

[81] BenAbdelkader, C., Cutler, R., & Davis, L. 2002. Stride and cadence as a biometric in automatic person identification and verification. In *Proc. Fifth IEEE Int Automatic Face and Gesture Recognition Conf*, 372–377.

[82] Wang, L., Tan, T., Ning, H., & Hu, W. 2003. Silhouette analysis-based gait recognition for human identification. 25(12), 1505–1518.

[83] Cunado, D., Nixon, M., & Carter, J. 1997. Using gait as a biometric, via phase-weighted magnitude spectra. In *Audio- and Video-based Biometric Person Authentication*, Bigün, J., Chollet, G., & Borgefors, G., eds, volume 1206 of *Lecture Notes in Computer Science*, 93–102. Springer Berlin / Heidelberg. 10.1007/BFb0015984.

[84] Rustagi, L., Kumar, L., & Pillai, G. N. 2009. Human gait recognition based on dynamic and static features using generalized regression neural network. In *Proc. Second Int. Conf. Machine Vision ICMV '09*, 64–68.

[85] Singh, J. P. & Jain, S. 2010. Person identification based on gait using dynamic body parameters. In *Proc. Trendz in Information Sciences & Computing (TISC)*, 248–252.

[86] Jensen, R., Paulsen, R., & Larsen, R. 2009. Analyzing gait using a time-of-flight camera. In *Image Analysis*, volume 5575 of *Lecture Notes in Computer Science*, 21–30. Springer Berlin – Heidelberg.

[87] Buttgen, B. & Seitz, P. july 2008. Robust optical time-of-flight range imaging based on smart pixel structures. *IEEE Transactions on Circuits and Systems I*, 55(6), 1512 –1525.

[88] ud Din, A., Halin, I. A., & Shafie, S. B. 2009. A review on solid state time of flight tof range image sensors. In *Proc. IEEE Student Conf. Research and Development (SCOReD)*, 246–249.

[89] Chiabrando, F., Chiabrando, R., Piatti, D., & Rinaudo, F. 2009. Sensors for 3d imaging: Metric evaluation and calibration of a ccd/cmos time-of-flight camera. *Sensors*, 9(12), 10080–10096.

[90] Bhatti, A. 2008. *Stereo Vision*. InTech.

[91] Oprisescu, S., Burlacu, C., & Buzuloiu, V. june 2010. Action recognition using time of flight cameras. In *8th International Conference on Communications (COMM), 2010*, 153 –156.

[92] Hussmann, S. & Hess, H. 2006. Dreidimensionale umwelterfassung. volume Issue 8, pp 55–59. WEKA Publisher House.

[93] Kahlmann, T., Remondino, F., & Ingens, H. 2006. Calibration for increased accuracy of the range imaging camera swissranger tm.

[94] Falie, D. & Buzuloiu, V. 2008. Wide range time of flight camera for outdoor surveillance. In *Proc. Microwaves, Radar and Remote Sensing Symp. MRRS 2008*, 79–82.

[95] Falie, D. & Buzuloiu, V. july 2007. Noise characteristics of 3d time-of-flight cameras. In *International Symposium on Signals, Circuits and Systems, 2007. ISSCS 2007.*, volume 1, 1 –4.

[96] Steiger, O., Felder, J., & Weiss, S. oct. 2008. Calibration of time-of-flight range imaging cameras. In *15th IEEE International Conference on Image Processing (ICIP).*, 1968 –1971.

[97] W. Karel, S. Ghuffar, N. P. 2010. Quantifying the distortion of distance observations caused by scattering in time-of-flight range cameras. *The International Archives Of The Photogrammetry, Remote Sensing And Spatial Information Sciences*, XXXVIII/5, 316 – 321.

[98] Lottner, O., Sluiter, A., Hartmann, K., & Weihs, W. 2007. Movement artefacts in range images of time-of-flight cameras. In *Proc. Int. Symp. Signals, Circuits and Systems ISSCS 2007*, volume 1, 1–4.

[99] Ng, H., Tan, W.-H., Tong, H.-L., Abdullah, J., & Komiya, R. 2009. Extraction and classification of human gait features. In *Visual Informatics: Bridging Research and Practice*, volume 5857 of *Lecture Notes in Computer Science*, 596–606. Springer Berlin-eidelberg. 10.1007-978-3-642-05036-7-56.

[100] Otsu, N. jan. 1979. A threshold selection method from gray-level histograms. *Systems, Man and Cybernetics, IEEE Transactions on*, 9(1), 62 –66.

[101] Haralick, R. M., Sternberg, S. R., & Zhuang, X. july 1987. Image analysis using mathematical morphology. *IEEE Transactions on Pattern Analysis and Machine Intelligence,*, PAMI-9(4), 532 –550.

[102] Guo, Y., Xu, G., & Tsuji, S. 1994. Tracking human body motion based on a stick figure model. 5, 1–9.

[103] Holien, K. Gait recognition under non-standard circumstances. Master's thesis, M.Sc. in Information Security,Gjovik Univeristy College, 2008.

[104] Keogh, E. J. & Pazzani, M. J. 2001. Derivative dynamic time warping. In *In First SIAM International Conference on Data Mining (SDM 2001*.

[105] Wang, L., Tan, T., Hu, W., & Ning, H. sept. 2003. Automatic gait recognition based on statistical shape analysis. *Image Processing, IEEE Transactions on*, 12(9), 1120 – 1131.

[106] Derawi, M. O., Ali, H., , & Cheikh, F. A. 2011. Gait recognition using time-of-flight sensor. In *BIOSIG 2011, Darmstadt, Germany October 2011*.

A Participation agreement

Participant Agreement Declaration

Participation in acquisition of gait data

I am participating in the acquisition of gait data on a voluntarily basis. The data are taken using Time of Flight sensor to fulfill the purpose that is described in detail on the back side of this sheet. The data processing institutions are the Gjøvik University College (Høgskolen i Gjøvik). These institutions take care that the recorded data are solely used for teaching and research purposes. With my signature I confirm the following:

1. I have been informed in oral and written form about the content and purpose of the collected data that is in relation to my person.
2. My data will only be used to serve this purpose. The detailed description of the purpose is documented on the back side of this sheet.
3. I allow that gait data from me are collected.
4. I have been informed that I can reject to sign the agreement.
5. I have been informed that I can request to receive insight in the collected data before such data is used for teaching and research purposes.
6. I know that I can withdraw my participation anytime I want without giving any explanation and all data collected from we will be deleted permanently.

All data will be deleted respectively the link between the data and my name will be destroyed as soon as it is not necessary to maintain it. This will happen as the research experiment has been completed.

First name - family name: ______________________________
Gender: male /female
Meta information:
Age _________
Height (in cm)____________
Length of leg (in cm) _________
Kind of worn shoes _____________________________________
Time _________ Gjøvik, date ________________ signature: ____________________
2nd Session Time _________ , Gjøvik, date ________________

Background information for this agreement

From each participant we capture gait data while the participant is walking. Purpose of this project The data will be used for the following purpose: Provision of data to the biometric research groups in the Gjøvik University College. The data will be stored and analyzed without link to the name of the student but with the research relevant meta-data such as age and gender. Background information The recorded data will be used to develop and test methods which allow the authentication by gait recognition. User authentication can be obtrusive mission in access control. This shows the need for user-friendly authentication methods which enable an unobtrusive authentication. A second focus is on technology research for enabling privacy protection of the stored references (so called biometric templates) in a biometric system. Since biometric technologies are widely adopted in multiple applications, the threat of compromising the biometric templates becomes ever more serious. Based on earlier studies it is expected that this research will lead to new technological measures that allows for templates that prevent the possibility for cross-matching and associated data mining, and allows for renewability in case the biometric record is compromised. The data set will be used to validate the scientific research results. It will be taken care that no attempt is being made to analyze the captured signals regarding diseases or personal characteristics and habits of the subject. For the purpose of this research project it is only of relevance, whether or not recognition can be performed with high reliability.

B Filename convention

The feature files are named as follows. sessionID_subjectID_attemptID_FeatureID.txt

sessionID :identification number of sessions 1 and 2.

subjectID :identification number of subjects from 01 to 30.

AttemptID :identification number of attempts from 1 to 5.

FeatureID :identification number of the extracted features.

- Front shin (01).
- Back shin (02).
- Front thigh (03).
- Back thigh (04).